Doctoral Thesis

.

Involvement of lysophosphatidic acid-evoked TRPA1 and TRPV1 activation in peripheral itch sensation in mice

Hiroki Kittaka

Department of Physiological Sciences

School of Life Science

The Graduate University for Advanced Studies (SOKENDAI)

2013

Abstract

The sensation of itch, formally called pruritus is defined as ‘an unpleasant cutaneous sensation that provokes a desire to scratch’. So far, many pruritogens have been revealed to activate receptors or ion channels expressed in dorsal root ganglion (DRG) neurons that transmit itch sensation in the periphery. Some kinds of pruritus involved in pathophysiological conditions such as atopic dermatitis, uremia with hemodialysis and cholestasis are often resistant to antihistamines. This suggests that there are histamine-independent mechanisms, however, which have not been fully understood. Lysophosphatidic acid (LPA) is believed to be one of the molecules involved in the histamine-independent mechanisms (cholestatic pruritus in humans) and reported to induce itch-related and pain-related behaviors in mice. However, whether LPA induces itch, pain or both in the periphery is unclear. In addition, the cellular and molecular mechanisms of the LPA-induced itch and/or pain sensation are not elucidated.

First, I investigated whether LPA induces itch and/or pain using a cheek injection model to distinguish itch- and pain-related behaviors. LPA markedly induced itch-related scratching behaviors without increases in pain-related wiping behaviors in wild-type (WT) mice. The physiological role of LPA was suggested to induce itch sensation rather than pain sensation in the periphery in mice. Therefore, I examined the effect of LPA on mouse DRG neurons and how LPA affects the DRG neurons using a Ca^{2+}-imaging method. LPA robustly increased intracellular Ca^{2+} concentrations ($[Ca^{2+}]_i$) in approximately half of mouse DRG neurons, suggesting that DRG neurons directly responded to LPA. The $[Ca^{2+}]_i$ increases were abolished under an extracellular Ca^{2+}-free condition, suggesting that there were LPA-responding Ca^{2+}-permeable molecules expressed in the plasma membrane of DRG neurons. Transient receptor

potential ankyrin 1 (TRPA1) and vanilloid 1 (TRPV1) are Ca^{2+}-permeable non-selective cation channels, which are reported to be expressed in DRG neurons and contribute to the peripheral itch transduction. Therefore, the functional expressions of TRPA1 and TRPV1 in LPA-responding (LPA^+) DRG neurons were investigated by application of the selective agonists, allyl isothiocyanate and capsaicin, respectively. Approximately 90% of the LPA^+ DRG neurons functionally expressed TRPA1 and/or TRPV1. To further examine the involvement of TRPA1 and/or TRPV1 in the LPA actions, cells were treated with selective antagonists of TRPA1 and TRPV1 (A967079 and capsazepine, respectively) before application of LPA. As a result, both A967079 and capsazepine decreased LPA^+ neurons. To further clarify the contribution of TRPA1 and TRPV1 to the LPA-induced $[Ca^{2+}]_i$ increases, DRG neurons obtained from WT, TRPA1 knock-out (TRPA1KO), TRPV1KO and TRPA1/TRPV1 double KO (A1V1DKO) mice were used and I found that LPA^+ neurons were decreased in each of the KO strain. These results of the Ca^{2+}-imaging study suggested that LPA caused $[Ca^{2+}]_i$ increases through activation of both TRPA1 and TRPV1. Furthermore, I observed that LPA-induced scratching behaviors in a cheek-injection model were reduced in TRPA1KO, TRPV1KO and A1V1DKO mice, indicating that the LPA-induced scratching behaviors were TRPA1- and/or TRPV1-dependent, which was consistent with the results of the Ca^{2+}-imaging study. The LPA-induced $[Ca^{2+}]_i$ increases were inhibited by not only antagonists of TRPA1 and TRPV1 but also an LPA receptor antagonist (H2L 5765834), suggesting the possible signaling cascade to activate TRPA1 and/or TRPV1 after LPA receptor activation. Possibility of direct activation of TRPA1 by LPA was also examined by the inside-out patch-clamp recording of human embryonic kidney 293T cells expressing mouse TRPA1. Increases

in single channel openings upon LPA application in an excised membrane patch were observed, which indicated that TRPA1 can be directly activated by LPA in a membrane-delimited manner. These results indicated that there were direct and indirect pathways in the LPA-induced TRPA1 activation.

Taken together, I concluded that LPA induced itch-related scratching behaviors in a TRPA1- and/or TRPV1-dependent manner without increasing pain-related wiping behaviors and that LPA caused $[Ca^{2+}]_i$ increases in DRG neurons through TRPA1 and/or TRPV1 activation. I also found that LPA directly activated TRPA1 and that LPA could activate TRPA1 and/or TRPV1 through some signaling cascade after LPA receptor activation as well. The results presented in this study suggest that the action of LPA on TRPA1 could be involved in the peripheral itch signaling in humans. Thus, it is intriguing to speculate that antagonizing TRPA1 or TRPV1 function could lead to novel anti-itch therapies.

1. Abbreviations

AA	arachidonic acid
AITC	allyl isothiocyanate
ATX	autotaxin
A1V1DKO	TRPA1 and TRPV1 double-knockout
$[Ca^{2+}]_i$	intracellular calcium concentration
CGRP	calcitonin gene-related peptide
COX	cyclooxygenase
cryo-EM	cryo-electron microscopy
DAG	diacylglycerol
DMEM	Dulbecco's modified Eagle's medium
DRG	dorsal root ganglion
EC_{50}	50% effective concentration
ER	endoplasmic reticulum
FBS	fetal bovine serum
GPCR	G protein-coupled receptor
HEK293T	human embryonic kidney 293T
H1	histamine receptor 1
IP_3	inositol 1,4,5-trisphosphate
LPA	lysophosphatidic acid
LOX	lipoxygenase
LT	leukotriene
lysoPLD	lysophospholipase D
mGluR5	metabotropic glutamate receptor 5
MrgprA3	Mas-related g protein-coupled receptor A3
Nppb	natriuretic polypeptide b
NP_o	number of channels × open probability
PAR2	protease activated receptor 2
PBC	primary biliary cirrhosis
PG	prostaglandin
PH-like domain	plekstrin homology-like domain
PIP_2	phosphatidylinositol 4,5-bisphosphate
PLA_2	phospholipase A_2
PLC	phospholipase C
PTX	pertussis toxin

SNL	sciatic nerve ligation
TM	transmembrane domain
TRPA1	transient receptor potential ankyrin 1
TRPA1KO	TRPA1-knockout
TRPV1	transient receptor potential vanilloid 1
TRPV1KO	TRPV1- knockout
TSLP	thymic stromal lymphopoietin
TX	thromboxane
WT	wild type
5-HT	5-hydroxytryptamine
5-(S)-HETE	5-(S)-hydroxyeicosatetraenoic acid
12-(S)-HPETE	12-(S)-hydroperoxyeicosatetraenoic acid
$15dPGJ_2$	15-deoxyprostaglandin J_2
Δ^{12}-PGJ_2	Δ^{12}- prostaglandin J_2

Table of contents

2. Introduction

2.1 Peripheral itch system

The sensation of itching, formally called pruritus is defined as ‘an unpleasant cutaneous sensation that provokes a desire to scratch’ (Rothman, 1941). Itching can be separated into two classes: peripheral (dermal or neuropathic) and central (neuropathic, neurogenic or psychogenic) (Twycross et al., 2003). Current understanding of the peripheral itch pathway is as follows. When a subset of C-fibers, originating superficially in the skin, is activated by a pruritogen that invokes an itching sensation, the impulses are transmitted to the dorsal horn neurons of the spinal cord through the spinothalamic tract to the thalamus, and to the somatosensory cortex (Twycross et al., 2003, Ikoma et al., 2006, Davidson et al., 2010).

Histamine is the most-studied pruritogen. It evokes peripheral itching sensations in humans (Sikand et al., 2011) and induces itch-related behaviors in mice (Shimada et al., 2008). Based on these facts, H1-antihistamines such as diphenhydramine are often used and are effective for pruritic patients. However, there are cases in which H1-antihistamines are ineffective, e.g., atopic dermatitis, uremia with hemodialysis and cholestasis (Twycross et al., 2003). The latter cases of pruritus imply that unknown histamine-independent mechanisms could be at work. Several histamine-independent mechanisms have been proposed. These mechanisms include (1) a PAR2-TSLP (thymic stromal lymphopoietin) system in atopic dermatitis (Wilson et al., 2013b), (2) involvement of κ-opioid receptors in hemodialysis (Wikstöm et al., 2005) and (3) lysophosphatidic acid (LPA)-mediated itching identified in cholestatic pruritus (Kremer et al., 2010). Although all these mechanisms need to be examined further, it is well known that LPA causes scratching behaviors in mice, and the mechanism is not well

elucidated.

2.2 Lysophosphatidic acid and the involvement in pruritus

LPA is a small, ubiquitous phospholipid that plays important roles in cell survival, apoptosis, motility, shape formation, differentiation and other processes (Tigyi. 2010). LPA is known to activate at least 6 G protein-coupled receptors (LPA_1-LPA_6) (Tigyi, 2010) and some ion channels (Chemin et al., 2005; Nieto-Posadas et al., 2011). In a peripheral sensory system, LPA was reported to be an initiator of neuropathic pain in a sciatic nerve ligation (SNL) model (Inoue et al., 2004). In the SNL model, LPA activated LPA_1 (Inoue et al., 2004) or LPA_5 (Lin et al., 2012) and caused a demyelination of the sciatic nerve followed by a decrease in pain threshold. In addition, LPA was reported to be an endogenous pruritogen in cholestatic patients with pruritus (Kremer et al., 2010). The itching intensity was correlated to the serum level of the LPA-producing enzyme, autotaxin (ATX). However, it is not known how ATX is initially up-regulated in cholestasis or how LPA activates primary sensory neurons.

2.3 Transient receptor potential channels involved in itching sensations

The first transient receptor potential (TRP) gene was discovered in a study of a mutant *Drosophila melanogaster* strain with an abnormality in photosensing (Cosens et al., 1969) and the gene was later named *trp* (Minke et al., 1975). *trp* was cloned (Montell et al., 1989) and shown to be a calcium-permeable channel (Hardie et al., 1992). Thereafter rodent TRP homologs were explored, and they currently constitute the TRP channel superfamily consisting of 6 subfamilies (ankyrin, canonical, melastatin, mucolipin, polycystin and vanilloid) including a total of 28 channels (TRPA1, TRPC1 -

7, TRPM1 - 8, TRPML1 - 3, TRPP1 - 3, and TRPV1 - 6). Human TRP channels are composed of 27 channels because *TRPC2* is a pseudo gene (Gees et al., 2012).

Of all the TRP channels, TRPA1 (Wilson et al., 2011), TRPV1 (Shim et al., 2007) and TRPV3 (Yoshioka et al., 2009) have been reported to be involved in pruritus. TRPA1 and TRPV1 are expressed in DRG neurons. They are greatly important to the physiology of pruritus in addition to pain sensation. On the other hand, the involvement of TRPV3 in pruritus is due to a spontaneous gain-of-function mutation in the skin (Yoshioka et al., 2009). In addition to their roles as sensors for painful stimuli (Julius, 2013), recent studies have shown that both channels are also essential for the sensation of itching (Fernandes et al., 2013; Cevikbas et al., 2013).

TRPA1 was identified initially as a molecule responding to noxious cold stimuli. TRPA1 is expressed in peptidergic, CGRP-positive DRG neurons (Story et al., 2003). Since then TRPA1 has been recognized as the receptor for pain sensation caused by inflammation (Bautista et al., 2013) or various irritants such as AITC (Jordt et al., 2004), formalin (McNamara et al., 2007), hydroxide ions (Fujita et al., 2008), and other agents (Nilius et al., 2012). The role of TRPA1 in pruritus was reported by Wilson et al. in 2011. They showed that pruritus induced by chloroquine, an antimalarial drug, is dependent on activation of TRPA1 but not TRPV1 following the activation of the chloroquine receptor MrgprA3 (Liu et al., 2009). Recently, pruritus induced in a dry-skin model (Wilson et al., 2013a) and by cytokine TSLP produced in atopic dermatitis (Wilson et al., 2013b) was reported to be TRPA1-dependent.

TRPV1 was discovered as a capsaicin receptor that was also activated by noxious heat stimuli (Caterina et al., 1997), protons (Tomimaga et al., 1998) and many other compounds (Winter et al., 2013). TRPV1 is now largely accepted as one of the most

important molecules involved in pain sensation (Julius, 2013). Similar to TRPA1, TRPV1 is involved in pruritus mediated by several substances (Imamachi et al., 2009) including histamine (Shim et al., 2007), trypsin (Costa et al., 2008) and natriuretic polypeptide b (Mishra et al., 2013), although the involvements of TRPA1 in such pruritus haven't been well investigated.

The peripheral mechanism of pruritus involving TRPA1 and/or TRPV1 appears to be very complex. For example, several intracellular signals following the activation of multiple pruritogenic receptors have been reported. In this study, I hypothesized that LPA activates primary sensory neurons through TRPA1 and/or TRPV1. Moreover, this study examined the physiological role and the mechanism of the involvement of LPA.

3. Methods and Materials

Animals－Male C57BL/6NCr mice (6 - 10 weeks old; SLC, Japan) were housed in a controlled environment (12 h light/dark cycle; 22-24℃; 50 - 60% humidity) with food and water provided *ad libitum*. TRPA1-KO and TRPV1-KO mice were kindly provided by Dr. David Julius (University of California, San Francisco). TRPA1/TRPV1 double KO (A1V1DKO) mice were obtained by crossbreeding TRPA1KO and TRPV1KO mice. All the TRPA1KO, TRPV1KO and A1V1DKO mice used in this study were on a C57BL/6NCr background. All procedures involving and care and use of animals were approved by the institutional Animal Care and Use Committee of National Institute of Natural Sciences and carried out in accordance with the National Institutes of Health *Guide for the care and use of laboratory animals* (NIH publication No. 85-23. Revised, 1985).

Behavioral test－A cheek injection model (Shimada et al., 2008) was used in this study. After a 30-min habituation, 10 μl of saline as a vehicle or LPA (Avanti Polar Lipids, USA) dissolved in saline (100 nmol/10 μl) was intradermally injected into the right cheek of the mice with a 30-gauge needle (BD, USA) coupled to a Hamilton syringe by PE-10 tube and behaviors were recorded for 30 min. Thereafter, scratching and wiping responses toward the injection site were counted. Scratching responses were defined as serial movements in which a mouse lifted its hindpaws for scratching and subsequently returned the hindpaws to the floor or to the mouth. Wiping behaviors were defined as only unilateral behaviors with the forelimb as distinguished from grooming behaviors.

Cultures of dissociated DRG neurons—Dorsal root ganglia from all spinal levels of adult C57BL/6NCr mice were rapidly dissected and dissociated by incubation for 20 min at 37℃ in Earle's balanced salt solution (EBSS, Sigma) containing 10% fetal bovine serum (FBS; Biowest, France), 2 mM L-glutamine (GulutaMAX, Gibco), 1% vitamin mixture, 50 U ml^{-1} penicillin/ 50 μM ml^{-1} streptomycin (Invitrogen) and 2.5 mg/ml collagenase (C7657, Sigma). After changing the salt solutions by centrifugation (RT, 1000 rpm, 4 min), DRG were gently triturated with a fire-polished Pasteur pipette and filtered through 70 μm nylon mesh (BD). The solution was changed to Dulbecco's modified Eagle's medium (DMEM, Wako, Japan) containing 10% FBS, 50 U ml^{-1} penicillin/ 50 μM ml^{-1} streptomycin and 2 mM L-glutamine. DRG neurons were re-suspended in DMEM, inoculated in a drop on poly-D-lysine (100 μg/ml, Sigma) pre-coated coverslips and incubated for 30 min at 37℃ in 5% CO_2 followed by medium addition. DRG neurons were used in 14-24 h after dissection.

Calcium imaging—Calcium-imaging experiments were conducted with the fluorescent indicator Fura 2-acetoxymethyl ester (Fura 2-AM; Molecular Probes). DRG neurons were incubated for 30 min in medium containing 5 μM Fura 2. Fura 2 fluorescence was measured under conditions in which a coverslip was set in a recording chamber and was perfused with a standard bath solution containing 140 mM NaCl, 5 mM KCl, 2 mM $MgCl_2$, 2 mM $CaCl_2$, 10 mM HEPES and 10 mM D-glucose at pH 7.4 adjusted with NaOH. Ca^{2+}-free bath solution was prepared by omitting 2 mM $CaCl_2$ from the solution and adding 5 mM EGTA. Ionomycin (5 μM) was applied to confirm cell viability. Fura 2 loaded in the cells was excited with 340- and 380- nm wavelength and emission was monitored at 510 nm with a digital CCD camera (ORCA-

HR C4742-95-12HR, Hamamatsu Photonics, Japan). Data were analyzed by using *ImageJ* software (National Institute of Health); values of the (340/380) ratio were normalized following the formula,

$$\Delta F_{Norm} = \{\text{ratio } (340/380) - \text{ratio } (340/380)_{Initial}\}/(\Delta F_{Ionomycin} - \text{ratio } (340/380)_{Initial})$$

ΔF_{Norm}: a normalized ratio (340/380) value. ratio $(340/380)_{Initial}$: an averaged ratio (340/380) value for the first 25 sec of an experiment. $\Delta F_{Ionomycin}$: subtraction of the averaged ratio (340/380) value for 25 sec before the ionomycin application, from the maximal ratio (340/380) value during ionomycin application for 100 sec. In this study, a response to application with $\Delta F_{Norm} \geq 0.1$ was defined as positive. Cells not responding to KCl (100 mM) application were regarded as non-neuronal cells.

Construction of mutant mouse TRPA1 ― mTRPA1 cDNA in the pcDNA5/FRT expression vector was used. Vectors containing the full-length mouse TRPA1 mutants were constructed by PCR with synthesized oligonucleotide primer sets that have specific substitutions that cause amino acid substitutions. Primer sets used in this study are shown in Table 1. The entire sequences including the desired substitutions in the mutants were confirmed by DNA sequencing.

Maintenance and transient transfection of HEK293T cells―Human embryonic kidney 293T (HEK293T) cells were maintained at 37℃ in 5% CO_2 in the supplemented DMEM described above. Transient transfection of HEK293-cells was achieved in PLUS™ Reagent (Invitrogen), Lipofectamine™ Regent (Invitrogen) and Opti-MEM® I Reduced Serum medium (Invitrogen) following the manufacturer's protocol. 0.5 μg mTRPA1 or mutated mTRPA1 in the pcDNA5/FRT and 0.1μg pGreen Lantern 1 were

transfected into HEK293T cells.

Electrophysiology－HEK293T cells expressing mTRPA1 or mutant mTRPA1 were used for single channel recording with standard patch pipettes (3-5 MΩ resistance) made of borosilicate glass capillaries (Harvard Apparatus). Before membrane excision, cells were perfused with the standard bath solution. The solution was exchanged before the excision and the pipette solution contains 140 mM KCl, 5 mM EGTA and 10 mM HEPES at pH 7.4, adjusted with KOH. The membrane potential was clamped at +30 mV in an inside-out configuration. Data from a single-channel recording were sampled at 10 kHz and filtered at 2 kHz. Data were analyzed using pCLAMP 10.2 software (Molecular Devices, USA)

Statistics－All results are expressed as means ± sem. Statistical analysis was performed with Mann-Whitney U test or Kruskal-Wallis tests followed by Steel's tests. $p < 0.05$ was considered significant.

4. Results

4.1 Effects of LPA on mouse scratching behaviors

LPA can induce scratching responses (Hashimoto et al., 2004; Kremer et al., 2010) and pain-related responses in mice (Renbäck et al., 2000; Nieto-Posadas et al., 2011), indicating the ambiguity of LPA actions in mice. In order to clarify the physiological role of LPA in mice, a cheek-injection model (Shimada et al., 2008) was chosen. Most compounds can be distinguished appropriately as either pruritogens or as algogens that evoke pain sensations (Akiyama et al., 2010a). Intradermal injection of LPA (100 nmol/10 μl/site) into the right cheek of mice was performed, followed by counting scratching and wiping behaviors. LPA markedly induced scratching responses but not wiping behaviors compared with vehicle-treatment (Fig. 1a and 1b). Figure 1c and 1d represent time courses of the behavior tests. The LPA-induced scratching responses peaked 16 - 20 min after injection. Thus, it was confirmed that LPA caused itching sensations upon injection into the mouse cheek.

4.2 Effects of LPA on intracellular Ca^{2+} concentrations in mouse DRG neurons

To examine whether LPA directly affected mouse DRG neurons, the cells were examined using a Ca^{2+}-imaging method. Application of 5 μM of LPA robustly increased intracellular Ca^{2+} concentrations ($[Ca^{2+}]_i$) in DRG neurons (Fig. 2a). Overall, 45.2 ± 5.5 % of total neurons (n = 213/500) were LPA-responding (LPA^+) (Fig. 2b). This effect was LPA dose-dependent, and the EC_{50} values for the proportion and the intensity (ΔF_{Norm}, see Methods and Materials) of LPA^+ neurons were 3.34 μM (Fig. 2c) and 1.07 μM (Fig. 2d), respectively. The LPA-induced $[Ca^{2+}]_i$ increases were not observed when the extracellular bath solution was free of Ca^{2+}, indicating that the

LPA-induced $[Ca^{2+}]_i$ increases were caused by Ca^{2+} influx from the extracellular space (Fig. 3a). It has been suggested that TRPA1 and/or TRPV1 and Ca^{2+} influx were involved in signaling associated with peripheral pruritus (Liu et al., 2013). To identify the DRG neuron subpopulation sensitive to LPA, selective agonists for TRPA1 (100 μM AITC) and TRPV1 (1 μM capsaicin) were applied after LPA (Fig. 3b). DRG neurons were divided into eight subpopulations composed of four groups: LPA^+, AITC-responding ($TRPA1^+$), capsaicin-responding ($TRPV1^+$), and others (Fig. 3c). LPA^+, $TRPA1^+$ and $TRPV1^+$ subpopulations overlapped one another. Among the LPA^+ neurons, most (87.2 ± 2.7 %, 184/213, Fig. 3c) functionally expressed TRPA1 and/or TRPV1, suggesting that TRPA1 and/or TRPV1 contributed to the effect of LPA on DRG neurons. Changes in the intensities and the times to the peak $[Ca^{2+}]_i$ increases in the LPA^+ neurons were not different among $LPA^+/TRPA1^+/TRPV1^+$, $LPA^+/TRPA1^+$, $LPA^+/TRPV1^+$ and LPA^+ alone groups (Fig. 3d and 3e). To examine whether activation of TRPA1 and/or TRPV1 was involved in the $[Ca^{2+}]_i$ increases induced by LPA application, a TRPA1 inhibitor (1 μM A967079) or a TRPV1 inhibitor (10 μM capsazepine) was applied before LPA application (Fig. 4a and 4b). Among the LPA^+ neurons, application of both inhibitors significantly decreased LPA^+ neurons (Fig. 4c and 4d), suggesting that activation of both TRPA1 and TRPV1 was involved in the LPA-induced $[Ca^{2+}]_i$ increases.

In order to further clarify the contribution of TRPA1 and/or TRPV1 to LPA-responsiveness, TRPA1KO and/or TRPV1KO DRG neurons were used. LPA^+ neurons were significantly ($P < 0.05$) decreased in TRPA1KO and/or TRPV1KO DRG neurons (TRPA1KO: 26.0 ± 6.0% (144/579), TRPV1KO: 20.3 ± 2.8% (93/443), and A1V1DKO: 13.5 ± 3.2% (65/455)). Taken together (Fig. 4e), it was concluded that

most of the LPA-induced $[Ca^{2+}]_i$ increases in DRG neurons occurred through activation of TRPA1 and/or TRPV1.

4.3 Involvement of TRPA1 and TRPV1 in LPA-induced scratching responses in mice

To examine the contribution of TRPA1 and/or TRPV1 to the LPA-induced scratching responses, LPA was injected into the cheek of WT, TRPA1KO, TRPV1KO and A1V1DKO mice. Scratching behaviors decreased in the TRPA1KO, TRPV1KO and A1V1DKO mice to a level similar to that of the vehicle-treated group with similar time courses. No changes in the wiping behaviors were observed in the four mouse strains (Fig. 5a-d), suggesting both TRPA1 and TRPV1 were involved in the LPA-induced scratching behaviors.

4.4 Involvement of LPA receptors in LPA-induced increases of intracellular Ca^{2+} concentrations in DRG neurons

At least 6 G protein-coupled LPA receptors have been reported (LPA_1 - LPA_6, Mutoh et al., 2012). Among them, LPA_1, LPA_3 and LPA_5 are expressed in DRG neurons (Inoue et al., 2004; Oh et al., 2008). These three receptors were reported to induce intracellular Ca^{2+} increases (Ohta et al., 2003; Bandoh et al., 1999; Lee et al., 2006). To investigate the involvement of these LPA receptors in the LPA-induced $[Ca^{2+}]_i$ increases in DRG neurons, H2L 5765384 (an antagonist of LPA_1, LPA_3 and LPA_5, Williams et al., 2009) was used. Ten μM of H2L 5765834 inhibited the LPA-induced $[Ca^{2+}]_i$ increases in 78.0 ± 6.8% (79/95) of the LPA^+-DRG neurons (Fig 6a-c), 71.5 ± 4.3 % of which (61/79) expressed TRPA1 and/or TRPV1, suggesting possible involvement of LPA receptors in the LPA-induced $[Ca^{2+}]_i$ increases in DRG neuron. It

was also checked whether H2L 5765834 inhibits $[Ca^{2+}]_i$ increases induced by AITC or capsaicin. H2L 5765834 didn't inhibit the action of both chemicals (Fig. 7a and 7b), suggesting that H2L 5765834 doesn't affect functions of TRPA1 or TRPV1. In the presence of H2L 5765834 (10 μM), the proportions of the AITC-responding and capsaicin-responding neurons were 61.9 ± 5.4% (159/247) and 74.1 ± 3.0% (149/201), respectively (Fig 7c), a little higher than the proportions of $TRPA1^+$- and $TRPV1^+$-DRG neurons in the experiments shown in Fig. 3c ($TRPA1^+$: 49.9 ± 5.7% and $TRPV1^+$: 59.6 ± 2.7%) probably due to the lack of preapplication of LPA.

4.5 Direct activation of TRPA1 by LPA

Direct activation of TRPV1 by LPA binding was shown by the recordings of macroscopic currents in inside-out membrane patches excised from TRPV1-expressing HEK293 cells (Nietro-Posadas et al., 2011). Here, it was hypothesized that LPA could directly activate TRPA1 similar to TRPV1. Thus, single channel recordings were performed in inside-out membrane patches excised from mouse TRPA1-expressing HEK293T cells. LPA application (1-10 μM) induced opening of the single-channel currents at +30 mV in a dose-dependent manner (Fig. 8a), indicating that LPA activated TRPA1 in a membrane-delimited manner. The LPA-activated currents were inhibited almost completely by the application of 1 μM A967079, a specific TRPA1 inhibitor (Fig. 8b), further indicating the activation of TRPA1 by LPA. The unitary amplitudes of the 5 μM LPA-activated currents at the same membrane potential were similar to the unitary amplitudes of the currents activated by a TRPA1-specific agonist, AITC (100 μM) (3.31 ± 0.73 pA and 3.74 ± 0.55 pA, respectively (Fig. 8c)). These results also indicated that LPA activated TRPA1.

4.6 Identification of the amino acids involved in the LPA-mediated activation of TRPA1

In order to explore the amino acid residues involved in LPA-mediated activation of TRPA1, the following observation were taken into consideration. First, the amino acid residue involved in TRPV1 activation by LPA was identified as Lysine710 (K710) located in the intracellular C-terminal region (Nietro-Posadas et al., 2011). This amino acid is shared by the action of the important signaling phospholipid, phosphatidylinositol 4,5-bisphosphate (PIP_2) (Brauchi et al., 2008). Second, structural interaction between TRPV1 and PIP_2 was investigated in a 3D modeling study, and the results suggested that several positively-charged amino acid residues including K710 located in the subcellular space of the channel interacted with PIP_2 (Brauchi et al., 2008). Third, the region that contains the amino acid is a 'TRP domain' found among the TRPC, TRPM and TRPV subfamilies (Rohacs et al., 2005) and some of them were experimentally shown to interact with PIP_2 via TRP domains (Nilius et al., 2008). Based on these reports, a putative consensus sequence was proposed and termed a 'PH-like domain' defined as [K/R]-X_{3-11}-[K/R]-X-[K/R]-[K/R] (R: arginine; X: any amino acid) (Nilius et al., 2008). Although TRPA1 regulation by PIP_2 was previously reported (Karashima et al., 2008; Kim et al., 2008), the detailed effects of PIP_2 on TRPA1 and the existence of a TRP domain in TRPA1 have not been established. Four PH-like domains have been proposed (Karashima et al., 2008) and the expected TRPA1 structure in the cryo-EM study showed that long ankyrin repeat domains hang in intracellular space (Cvetkov et al., 2011).

Taking this background into consideration, it was suggested that the residues responsible for LPA-TRPA1 interaction might be located around the subcellular region

of the transmembrane domains of TRPA1 in which basic residues are included (Fig. 9). This study focused on PH-like 3 and 4 regions and the K/R-rich regions located downstream of TM6 and other serial K/R residues. In total, 26 K or R residues were chosen as candidates for LPA action in TRPA1. Single or double mutants were constructed in which K or R residues were replaced with Q (glutamine) (Fig. 10a). Then, single-channel activation upon LPA application was studied in HEK293T cells expressing WT or mutant TRPA1 channels. Although one mutant, K592Q was not functional, all the other mutants provided single-channel openings upon application of known TRPA1 agonists. The functions of the mutant TRPA1 channels in the Ca^{2+}-imaging experiments were confirmed as well. Among the mutants tested, two mutants (KK672-673QQ and KR977-978QQ) showed markedly reduced NP_o values upon LPA application (0.09 ± 0.05 and 0.13 ± 0.04, respectively) compared with WT TRPA1 (0.35 ± 0.07, $P < 0.01$ (Fig. 10b)). The two mutants showed similar large responses to other known TRPA1 agonists, carvacrol (500 μM) and AITC (100 μM) (Fig. 8c), suggesting that these four basic residues were involved in the activation of TRPA1 by LPA. The KK672-673 and KR977-978 mutations were located in the proximal N- and C-terminal regions of TRPA1, respectively, suggesting that LPA activated TRPA1 through the interaction with multiple sites and that the two regions could be located close to one another.

5. Discussion

Pruritus in rodents has been evaluated by quantifying scratching behaviors induced by the injection of pruritogens into the back, a response that is not induced by algogens (Kuraishi et al., 1995). Although this method is very useful when studying known pruritogens, injection of capsaicin also can induce scratching responses in mice (Shimada et al., 2008), suggesting that scratching of the back (and neck) in rodents could be unsuitable for evaluating the ability of new compounds to cause pruritus. An alternative cheek-injection model was recently proposed. It has been used in a number of studies of pruritus (Akiyama et al., 2010a; Han et al., 2013; Roberson et al., 2013; Wilson et al., 2013a and 2013b). LPA causes scratching behaviors (Hashimoto et al., 2004; Kremer et al., 2010), as well as licking behaviors (Nieto-Posadas et al., 2011), resulting in a controversy whether the physiological role of LPA is to induce itching and/or pain. In the preceding studies, LPA was injected into the back and hind paws of mice to evaluate itch-related scratching behaviors and pain-related licking behaviors. In the present study, a cheek-injection model was utilized to clarify these issues and it was shown that LPA significantly induced itch-related scratching behaviors, but not pain-related wiping behaviors (Fig. 1a and 1b). These results have raised a question, i.e., why LPA induces licking behaviors (Nieto-Posadas et al., 2011). One explanation is that the evaluation of pain-related licking behaviors was not defined or distinguished well from biting behaviors in the experiments. Since licking behaviors toward the hindpaws are generally induced by algogens and biting behaviors toward the same region can be induced by pruritogens, they are not readily discriminated. Well-defined biting behaviors toward the hindpaws have been reported in a dry-skin itch-model (Akiyama et al., 2010b) or induced by an intraplantar injection of 5-HT (Hagiwara et al.,

1999), and they were both decreased by μ-opioid receptor antagonists, suggesting that biting behaviors toward the hindpaws are indeed itch-related. Because it is difficult to distinguish between licking and biting behaviors, considerable caution is necessary when analyzing compounds the effects of which are unestablished (Akiyama et al., 2013).

Peripheral targets of LPA are assumed to be mainly sensory nerve endings, keratinocytes or mast cells. In this study, the focus was on the effects of LPA on DRG neurons. LPA induced increases of $[Ca^{2+}]_i$ in DRG neurons and proportion of LPA^+-DRG neurons, which was dose-dependent (Fig. 2c and 2d). It was reported that plasma concentrations of LPA in healthy humans were in submicromolar levels (0.077 ± 0.026 μM in males and 0.103 ± 0.032 μM in females), less than the apparent threshold shown in Fig. 2c and 2d, and were correlated to the serum lysophospholipase D (lysoPLD) activity (Hosogaya et al., 2008). Therefore, LPA appeared not to induce $[Ca^{2+}]_i$ increases in DRG neurons in a healthy condition. Correlation between LPA concentrations the lysoPLD activity hasn't been examined yet in a study of cholestatic pruritus. Measurement of plasma LPA levels is very difficult because LPA is degraded easily by lipid phosphate phosphatases and because half-life of plasma LPA is about 3 min (Albers et al., 2010). However, good correlation between lysoPLD activity and itch intensity in cholestatic patients with pruritus (Kremer et al., 2010) suggests that LPA could be produced high enough to induce itch sensation in human with cholestasis. The mechanism by which LPA increases $[Ca^{2+}]_i$ is unknown, although LPA-mediated $[Ca^{2+}]_i$ increases were observed in rat DRG neurons (Elmes et al., 2004). This study is the first to show clarified that extracellular Ca^{2+} is necessary for the LPA-mediated $[Ca^{2+}]_i$ increases in mouse DRG neurons (Fig. 2a and 3a). These data suggest that

molecules associated with the plasma membrane are involved in Ca^{2+} influx. A recent study (Liu et al., 2013) proposed the involvement of Ca^{2+} influx through TRPA1 and/or TRPV1 in peripheral itch signaling. In the present analysis, experiments with agonists and antagonists for TRPA1 and/or TRPV1 revealed that the majority (~90%) of mouse DRG neurons functionally expressed TRPA1 and/or TRPV1 (Fig. 3b) and that activation of these two channels mediated the LPA-induced $[Ca^{2+}]_i$ increases (Fig. 4a and 4b). However, it is not clear which channel is more important for the LPA-induced $[Ca^{2+}]_i$ increases. They might contribute to the LPA-mediated $[Ca^{2+}]_i$ increases separately or in concert because there are several reports showing functional interaction between the two channels (Salas et al., 2009).

Consistent with the results that TRPA1 and TRPV1 were involved in the LPA-induced $[Ca^{2+}]_i$ increases in mouse DRG neurons, LPA-induced scratching behaviors were reduced in TRPA1KO, TRPV1KO and A1V1DKO mice (Fig. 5a and 5c), suggesting that both TRPA1 and TRPV1 were involved in the LPA-induced scratching responses. The fact that LPA-induced similar wiping behaviors in WT, TRPA1KO, TRPV1KO and A1V1DKO mice compared with vehicle-injected mice (Fig. 5b and 5d) suggests that LPA does not cause pain sensations in mice, at least in the cheek-injection model. LPA-induced scratching behaviors in TRPA1KO, TRPV1KO and A1V1DKO mice were reduced to levels similar to that of WT mice treated with control vehicle. Those results suggest that the functional interaction between TRPA1 and TRPV1 in causing scratching behaviors is similar to the results observed in the Ca^{2+}-imaging experiments.

One of the candidate targets of LPA action is an LPA receptor, which is supported by the fact that an LPA receptor antagonist inhibited the LPA-induced $[Ca^{2+}]_i$ increases

in DRG neurons (Fig. 6) while the LPA receptor antagonist did not inhibit the AITC- or capsaicin-induced $[Ca^{2+}]_i$ increases (Fig. 7). These results suggest the possible intracellular signaling to cause Ca^{2+} influx via TRPA1 and TRPV1 downstream of LPA receptor activation. LPA receptors are G protein-coupled receptors currently known as LPA_1-LPA_6. Diverse expressions of these receptors in various organs are reviewed in Choi et al., 2010. Among the 6 receptors, LPA_1, LPA_3 and LPA_5 were reported to be expressed in DRG neurons (Inoue et al., 2004; Oh et al., 2008). LPA_1 was identified as the first receptor for LPA (Hecht et al., 1996) and was reported to couple to $G_{i/o}$, $G_{q/11}$ and $G_{12/13}$ (Fukushima et al., 1998; Ishii et al., 2000). LPA_3 (Bandoh et al., 1999) was reported to couple to $G_{i/o}$, $G_{q/11}$ (Ishii et al., 2000), and LPA_5 was reported to couple to at least $G_{i/o}$ and $G_{q/11}$ (Lee et al., 2006). All these receptors couple to $G_{q/11}$/PLC (phospholipase C) signaling that is generally thought to be involved in intracellular Ca^{2+} release from the endoplasmic reticulum (ER) store. PLC hydrolyzes phosphatidylinositol 4,5-bisphosphate (PIP_2) into inositol 1,4,5-trisphosphate (IP_3) and diacylglycerol (DAG), and IP_3 activates ionotropic IP_3 receptor mainly expressed in ER, which releases Ca^{2+} into cytoplasm. However, Ca^{2+}-imaging experiments using DRG neurons in extracellular Ca^{2+}-free condition didn't represent $[Ca^{2+}]_i$ increases (Fig. 3a), suggesting that cytosolic Ca^{2+} release is not involved in the LPA-induced $[Ca^{2+}]_i$ increases. It could be needed to confirm that Ca^{2+} release from ER is not involved in the LPA-induced $[Ca^{2+}]_i$ increases by using ER Ca^{2+} scavenger, thapsigargin. Extracellular Ca^{2+}-dependent, LPA-induced $[Ca^{2+}]_i$ increases were reported in rat microglial cells that express at least LPA_3 (Möller et al., 2001). These $[Ca^{2+}]_i$ increases were insensitive to pertussis toxin (PTX), indicating the involvement of $G_{q/11}$/PLC signaling. Metabotropic glutamate receptor 5 (mGluR5) was reported to couple to

TRPV1 and induce $[Ca^{2+}]_i$ increases in a membrane-delimited manner (Kim et al., 2009). The $[Ca^{2+}]_i$ increases were sensitive to U73122, suggesting the involvement of PIP_2 hydrolysis or PLC action. In that work, the authors concluded that DAG could activate TRPV1 following mGluR5 and PLC activation. Similar mechanisms could be involved in the LPA-induced $[Ca^{2+}]_i$ increases in mouse DRG neurons observed in my study.

Pruritus induced by histamine, α-methyl-5-hydroxytryptamine and BAM8-22 were reported to be PLC-dependent (Han et al., 2006; Imamachi et al., 2009; Wilson et al., 2011). In addition, involvement of another phospholipase, phospholipase A_2 (PLA_2) in histamine-induced pruritus was reported (Kim et al., 2004; Shim et al., 2007), in which H1 receptor activation was followed by activation of PLA_2 and lypoxygenase (LOX). PLA_2 hydrolyzes membrane glycerophospholipids to arachidonic acids (AA) and lysophospholipids. AA is metabolized to prostaglandins (PGs), leukotrienes (LTs), thromboxanes (TXs), hydroperoxyeicosatetraenoic acids (HPETEs) and many other substances. LOX-dependent fatty acid metabolites such as 12-(S)-HPETE and 5-(S)-hydroxyeicosatetraenoic acid (5-(S)-HETE) were reported to directly activate TRPV1 (Hwang et al., 2000). Cyclooxygenase (COX)-dependent fatty acid metabolites such as $15dPGJ_2$ and Δ^{12}-PGJ_2 were reported to directly activate TRPA1 (Cruz-Orengo et al., 2008; Taylor

-Clark et al., 2008). Therefore, if PLA_2 is activated, following activation of LPA receptors, metabolites derived from AAs produced by PLA_2 could activate TRPA1 and TRPV1. However, activation of PLA_2 follow1ing GPCRs activity hasn't been well established. It would be definitely necessary to examine the involvement of PLA_2 in the LPA-induced activation of TRPA1 and TRPV1 by using PLA_2 inhibitors such as

quinacrine.

This study also asked another possibility that LPA directly activates TRPA1 or TRPV1 without involvement of LPA receptors. TRPV1 has already been reported to be directly activated by LPA and the involved amino acids were identified (Nieto-Posadas et al., 2011). Therefore, the present analysis focused on the effects of LPA on TRPA1. An experiment using heterologous expression of mouse TRPA1 in HEK293T cells might not be good for evaluating LPA actions on TRPA1, because this cell line endogenously expresses at least LPA_1 (Alderton et al., 2001) and LPA_5 (Nieto-Posadas et al., 2011), both of which were reported to induce $[Ca^{2+}]_i$ increases. Indeed, I confirmed that LPA induced $[Ca^{2+}]_i$ increases in naïve HEK293T cells in the absence of extracellular Ca^{2+}, suggesting the existence of $G_{q/11}$-mediated pathway. In addition, intracellular Ca^{2+} directly activates TRPA1 with interaction between Ca^{2+} and an N-terminal EF-hand domain (Zurborg et al., 2007; Doerner et al., 2007), which would make evaluation of the LPA's direct effect on TRPA1 difficult in the whole-cell recording. Therefore, I decided to do the single-channel recordings of the patch membrane excised from HEK293T cells expressing mouse TRPA1, which revealed that mouse TRPA1 was directly activated by LPA in a membrane-delimited manner (Fig. 8). The possible interaction between TRPA1 and LPA receptors could be hardly imagined in the inside-out configuration because LPA was applied to the intracellular side. Even when LPA applied to the intracellular side activates LPA receptors upon crossing the lipid bilayers, the downstream substances upon LPA receptor activation should not be abundant. Therefore, it is unlikely that LPA receptor activation causes TRPA1 channel opening in the inside-out configuration. In addition, the amino acid residues of TRPA1 interacting with LPA were identified as KK672-673 and KR977-978. This conclusion

was based on the results that the open probability was decreased upon LPA application while channel activation was preserved upon application of other TRPA1 agonists (carvacrol and AITC) in mutants in which those K or R residues were altered. Thus, I conclude that TRPA1 can be directly activated by LPA without involvement of LPA receptor activation. If that is the case, LPA should reach the intracellular action sites upon penetrating the lipid bilayers in the physiological conditions. Alternatively, LPA can be produced in the cytosol by the enzymes described above, in which upstream events would be necessary. Anyway, it is necessary to do the single-channel recording in the inside-out configuration with DRG neurons to confirm that direct activation of TRPA1 by LPA is true in native cells.

Because the identified residues were basic amino acids, it is possible that negatively charged LPA interacted with the positively charged lysine and arginine residues. The fact that both KK672 - 673 and KR977 - 978 are located close to the transmembrane domain in the N- and C-termini, respectively, suggests that those regions are close to one another in the functional protein. KR977 - 978 are in a region in which a TRP box is located in other TRP channels, a region that is reportedly involved in the action of PIP_2. In the case of TRPV1, PIP_2 that structurally contains LPA moiety acts on the region (Morales-Lázaro et al., 2013). These results suggest that these two basic regions are important for the action of lipid-like molecules with negative charges and could be involved in the interaction of PIP_2 and LPA with TRPA1. Indeed, TRPA1 has been reported to be regulated by PIP_2 (Karashima et al., 2008; Kim et al., 2008) although the structural basis has not been clarified. The four basic residues are conserved between mouse and human TRPA1, further supporting the importance of the residues for the TRPA1 function.

The results presented in this study suggest that the action of LPA on TRPA1 could be involved in the pathophysiological responses in humans. LPA has been identified as one of the most likely candidate pruritogens for cholestatic pruritus observed in diseases such as primary biliary cirrhosis (PBC). LPA concentrations between 1 and 10 μM (Fig. 2c and 2d) are attainable in cholestasis. Therefore, the LPA-induced itch-related behaviors observed in mice could explain the itch-sensation observed in such conditions in humans. PBC-model mice made with TRPA1KO or TRPV1KO strains could exhibit less itch-related behaviors. Although further experiments are necessary, it is possible that antagonizing TRPA1 or TRPV1 function could lead to novel anti-itch therapies.

6. References

Akiyama T, Carstens MI, Carstens E. (2010a) Facial injections of pruritogens and algogens excite partly overlapping populations of primary and second-order trigeminal neurons in mice. *J Neurophysiol*. **104**: 2442-50.

Akiyama T, Carstens MI, Carstens E. (2010b) Spontaneous itch in the absence of hyperalgesia in a mouse hindpaw dry skin model. *Neurosci Lett*. **484**: 62-5.

Akiyama T, Carstens E. (2013) Neural processing of itch. *Neuroscience*. **250**: 697-714.

Albers HM, Dong A, van Meeteren LA, Egan DA, Sunkara M, van Tilburg EW, Schuurman K, van Tellingen O, Morris AJ, Smyth SS, Moolenaar WH, Ovaa H. (2010) Boronic acid-based inhibitor of autotaxin reveals rapid turnover of LPA in the circulation. *Proc Natl Acad Sci U S A.* **107**: 7257-62.

Alderton F, Sambi B, Tate R, Pyne NJ, Pyne S. (2001) Assessment of agonism at G-protein coupled receptors by phosphatidic acid and lysophosphatidic acid in human embryonic kidney 293 cells. *Br J Pharmacol.* **134**: 6-9.

Bandoh K, Aoki J, Hosono H, Kobayashi S, Kobayashi T, Murakami-Murofushi K, Tsujimoto M, Arai H, Inoue K. (1999) Molecular cloning and characterization of a novel human G-protein-coupled receptor, EDG7, for lysophosphatidic acid. *J Biol Chem.* **274**: 27776-85.

Bautista DM, Pellegrino M, Tsunozaki M. (2013) TRPA1: A gatekeeper for inflammation. *Annu Rev Physiol*. **75**: 181-200.

Brauchi S, Orta G, Mascayano C, Salazar M, Raddatz N, Urbina H, Rosenmann E, Gonzalez-Nilo F, Latorre R. (2007) Dissection of the components for PIP2 activation and thermosensation in TRP channels. *Proc Natl Acad Sci U S A*. **104**: 10246-51.

Caterina MJ, Schumacher MA, Tominaga M, Rosen TA, Levine JD, Julius D. (1997) The capsaicin receptor: a heat-activated ion channel in the pain pathway. *Nature*. **389**: 816-24.

Cevikbas F, Wang X, Akiyama T, Kempkes C, Savinko T, Antal A, Kukova G, Buhl T, Ikoma A, Buddenkotte J, Soumelis V, Feld M, Alenius H, Dillon SR, Carstens E, Homey B, Basbaum A, Steinhoff M. (2013) A sensory neuron-expressed IL-31 receptor mediates T helper cell-dependent itch: Involvement of TRPV1 and TRPA1. *J Allergy Clin Immunol*. (in press).

Chemin J, Patel A, Duprat F, Zanzouri M, Lazdunski M, Honoré E. (2005) Lysophosphatidic acid-operated K+ channels. *J Biol Chem*. **280**: 4415-21.

Choi JW, Herr DR, Noguchi K, Yung YC, Lee CW, Mutoh T, Lin ME, Teo ST, Park KE, Mosley AN, Chun J. (2010) LPA receptors: subtypes and biological actions. *Annu Rev Pharmacol Toxicol.* **50**: 157-86.

Cosens DJ, Manning A. (1969) Abnormal electroretinogram from a Drosophila mutant. *Nature*. **224**: 285-7.

Costa R, Marotta DM, Manjavachi MN, Fernandes ES, Lima-Garcia JF, Paszcuk AF, Quintão NL, Juliano L, Brain SD, Calixto JB. (2008) Evidence for the role of neurogenic inflammation components in trypsin-elicited scratching behaviour in mice. *Br J Pharmacol*. **154**: 1094-103.

Cruz-Orengo L, Dhaka A, Heuermann RJ, Young TJ, Montana MC, Cavanaugh EJ, Kim D, Story GM. (2008) Cutaneous nociception evoked by 15-delta PGJ2 via activation of ion channel TRPA1. *Mol Pain.* **4**:30.

Cvetkov TL, Huynh KW, Cohen MR, Moiseenkova-Bell VY. (2010) Molecular architecture and subunit organization of TRPA1 ion channel revealed by electron microscopy. *J Biol Chem*. **286**: 38168-76.

Davidson S, Giesler GJ. (2010) The multiple pathways for itch and their interactions with pain. *Trends Neurosci*. **33**: 550-8.

Doerner JF, Gisselmann G, Hatt H, Wetzel CH. (2007) Transient receptor potential channel A1 is directly gated by calcium ions. *J Biol Chem.* **282**: 13180-9.

Elmes SJ, Millns PJ, Smart D, Kendall DA, Chapman V. (2004) Evidence for biological effects of exogenous LPA on rat primary afferent and spinal cord neurons. *Brain Res*. **1022**: 205-13.

Fernandes ES, Vong CT
, Quek S, Cheong J, Awal S, Gentry C, Aubdool AA, Liang L, Bodkin JV, Bevan S, Heads R, Brain SD. (2013) Superoxide generation and leukocyte accumulation: key elements in the mediation of leukotriene B_4-induced itch by transient receptor potential ankyrin 1 and transient receptor potential vanilloid 1. *FASEB J*. **27**: 1664-73.

Fujita F, Uchida K, Moriyama T, Shima A, Shibasaki K, Inada H, Sokabe T, Tominaga M. (2008) Intracellular alkalization causes pain sensation through activation of TRPA1 in mice. *J Clin Invest*. **118**: 4049-57.

Fukushima N, Kimura Y, Chun J. (1998) A single receptor encoded by vzg-1/lpA1/edg-2 couples to G proteins and mediates multiple cellular responses to lysophosphatidic acid. *Proc Natl Acad Sci U S A.* **95**: 6151-6.

Gees M, Owsianik G, Nilius B, Voets T. (2012) TRP channels. *Compr Physiol*. **2**: 563-608.

Hagiwara K, Nojima H, Kuraishi Y (1999) Serotonin-induced biting of the hind paw is itch-related response in mice. *Pain Res*. **14**:53–59.

Han L, Ma C, Liu Q, Weng HJ, Cui Y, Tang Z, Kim Y, Nie H, Qu L, Patel KN, Li Z, McNeil B, He S, Guan Y, Xiao B, Lamotte RH, Dong X. (2013) A subpopulation of nociceptors specifically linked to itch. *Nat Neurosci*. **16**: 174-82.

Hardie RC, Minke B. (1992) The trp gene is essential for a light-activated Ca2+ channel in Drosophila photoreceptors. *Neuron*. **8**: 643-51.

Hashimoto T, Ohata H, Momose K. (2004) Itch-scratch responses induced by lysophosphatidic acid in mice. *Pharmacology*. **72**: 51-6.

Hecht JH, Weiner JA, Post SR, Chun J. (1996) Ventricular zone gene-1 (vzg-1) encodes a lysophosphatidic acid receptor expressed in neurogenic regions of the developing cerebral cortex. *J Cell Biol.* **135**: 1071-83.

Hosogaya S, Yatomi Y, Nakamura K, Ohkawa R, Okubo S, Yokota H, Ohta M, Yamazaki H, Koike T, Ozaki Y. **(**2008) Measurement of plasma lysophosphatidic acid concentration in healthy subjects: strong correlation with lysophospholipase D activity. *Ann Clin Biochem.* **45**: 364-8.

Hwang SW, Cho H, Kwak J, Lee SY, Kang CJ, Jung J, Cho S, Min KH, Suh YG, Kim D, Oh U. (2000) Direct activation of capsaicin receptors by products of lipoxygenases: endogenous capsaicin-like substances. *Proc Natl Acad Sci U S A.* **97**: 6155-60.

Ikoma A, Steinhoff M, Ständer S, Yosipovitch G, Schmelz M. (2006) The neurobiology of itch. *Nat Rev Neurosci*. **7**: 535-47.

Imamachi N, Park GH, Lee H, Anderson DJ, Simon MI, Basbaum AI, Han SK. (2009) TRPV1-expressing primary afferents generate behavioral responses to pruritogens via multiple mechanisms. *Proc Natl Acad Sci U S A.* **106**: 11330-5.

Inoue M, Rashid MH, Fujita R, Contos JJ, Chun J, Ueda H. (2004) Initiation of neuropathic pain requires lysophosphatidic acid receptor signaling. *Nat Med*. **10**: 712-8.

Ishii I, Contos JJ, Fukushima N, Chun J. (2000) Functional comparisons of the lysophosphatidic acid receptors, LP(A1)/VZG-1/EDG-2, LP(A2)/EDG-4, and LP(A3)/EDG-7 in neuronal cell lines using a retrovirus expression system. *Mol Pharmacol.* **58**: 895-902.

Jordt SE, Bautista DM, Chuang HH, McKemy DD, Zygmunt PM, Högestätt ED, Meng ID, Julius D. (2004) Mustard oils and cannabinoids excite sensory nerve fibres through the TRP channel ANKTM1. *Nature*. **427**: 260-5.

Julius D. (2013) TRP channels and pain. *Annu Rev Cell Dev Biol*. **29**: 355-84.

Karashima Y, Prenen J, Meseguer V, Owsianik G, Voets T, Nilius B. (2008) Modulation of the transient receptor potential channel TRPA1 by phosphatidylinositol 4,5-biphosphate manipulators. *Pflugers Arch.* **457**: 77-89.

Kim BM, Lee SH, Shim WS, Oh U. (2007) Histamine-induced Ca(2+) influx via the PLA(2)/lipoxygenase/TRPV1 pathway in rat sensory neurons. *Neurosci Lett.* **361**: 159-62.

Kim D, Cavanaugh EJ, Simkin D. (2008) Inhibition of transient receptor potential A1 channel by phosphatidylinositol-4,5-bisphosphate. *Am J Physiol Cell Physiol*. **295**: C92-9.

Kim YH, Park CK, Back SK, Lee CJ, Hwang SJ, Bae YC, Na HS, Kim JS, Jung SJ, Oh SB. (2009) Membrane-delimited coupling of TRPV1 and mGluR5 on presynaptic terminals of nociceptive neurons. *J Neurosci.* **29**: 10000-9.

Kremer AE, Martens JJ, Kulik W, Ruëff F, Kuiper EM, van Buuren HR, van Erpecum KJ, Kondrackiene J, Prieto J, Rust C, Geenes VL, Williamson C, Moolenaar WH, Beuers U, Oude Elferink RP. (2010) Lysophosphatidic acid is a potential mediator of cholestatic pruritus. *Gastroenterology*. **139**: 1008-18.

Kuraishi Y, Nagasawa T, Hayashi K, Satoh M (1995) Scratching behavior induced by pruritogenic but not algesiogenic agents in mice. *Eur J Pharmacol*. **275**: 229-33.

Lee CW, Rivera R, Gardell S, Dubin AE, Chun J. (2006) GPR92 as a new G12/13- and Gq-coupled lysophosphatidic acid receptor that increases cAMP, LPA5. *J Biol Chem.* **281**: 23589-97.

Lin ME, Rivera RR, Chun J. (2012) Targeted deletion of LPA5 identifies novel roles for lysophosphatidic acid signaling in development of neuropathic pain. *J Biol Chem*. **287**: 17608-17

Liu Q, Tang Z, Surdenikova L, Kim S, Patel KN, Kim A, Ru F, Guan Y, Weng HJ, Geng Y, Undem BJ, Kollarik M, Chen ZF, Anderson DJ, Dong X. (2009) Sensory neuron-specific GPCR Mrgprs are itch receptors mediating chloroquine-induced pruritus. *Cell*. **139**: 1353-65.

Liu T, Ji RR. (2013) New insights into the mechanisms of itch: are pain and itch controlled by distinct mechanisms? *Pflugers Arch*. **465**: 1671-85.

Materazzi S, Nassini R, Andrè E, Campi B, Amadesi S, Trevisani M, Bunnett NW, Patacchini R, Geppetti P. (2008) Cox-dependent fatty acid metabolites cause pain through activation of the irritant receptor TRPA1. *Proc Natl Acad Sci U S A.* **105**: 12045-50.

McNamara CR, Mandel-Brehm J, Bautista DM, Siemens J, Deranian KL, Zhao M, Hayward NJ, Chong JA, Julius D, Moran MM, Fanger CM. (2007) TRPA1 mediates formalin-induced pain. *Proc Natl Acad Sci U S A.* **104**: 13525-30.

Minke B, Wu C, Pak WL. (1975) Induction of photoreceptor voltage noise in the dark in Drosophila mutant. *Nature*. **258**: 84-7.

Mishra SK, Hoon MA. (2013) The cells and circuitry for itch responses in mice. *Science*. **340**: 968-71.

Möller T, Contos JJ, Musante DB, Chun J, Ransom BR. (2001) Expression and function of lysophosphatidic acid receptors in cultured rodent microglial cells. *J Biol Chem.* **276**: 25946-52.

Montell C, Rubin GM. (1989) Molecular characterization of the Drosophila trp locus: a putative integral membrane protein required for phototransduction. *Neuron*. **2**: 1313-23.

Morales-Lázaro SL, Simon SA, Rosenbaum T. (2013) The role of endogenous molecules in modulating pain through transient receptor potential vanilloid 1 (TRPV1). *J Physiol*. **591**: 3109-21.

Mutoh T, Rivera R, Chun J. (2012) Insights into the pharmacological relevance of lysophospholipid receptors. *Br J Pharmacol.* **165**: 829-44.

Nieto-Posadas A, Picazo-Juárez G, Llorente I, Jara-Oseguera A, Morales-Lázaro S, Escalante-Alcalde D, Islas LD, Rosenbaum T. (2011) Lysophosphatidic acid directly activates TRPV1 through a C-terminal binding site. *Nat Chem Biol*. **8**: 78-85.

Nilius B, Owsianik G, Voets T. (2008) Transient receptor potential channels meet phosphoinositides. *EMBO J*. **27**: 2809-16.

Nilius B, Appendino G, Owsianik G. (2012) The transient receptor potential channel TRPA1: from gene to pathophysiology. *Pflugers Arch*. **464**: 425-58.

Oh DY, Yoon JM, Moon MJ, Hwang JI, Choe H, Lee JY, Kim JI, Kim S, Rhim H, O'Dell DK, Walker JM, Na HS, Lee MG, Kwon HB, Kim K, Seong JY. (2008) Identification of farnesyl pyrophosphate and N-arachidonylglycine as endogenous ligands for GPR92. *J Biol Chem.* **283**: 21054-64.

Ohta H, Sato K, Murata N, Damirin A, Malchinkhuu E, Kon J, Kimura T, Tobo M, Yamazaki Y, Watanabe T, Yagi M, Sato M, Suzuki R, Murooka H, Sakai T, Nishitoba T, Im DS, Nochi H, Tamoto K, Tomura H, Okajima F. (2003) Ki16425, a subtype-selective antagonist for EDG-family lysophosphatidic acid receptors. *Mol Pharmacol*. **64**: 994-1005.

Renbäck K, Inoue M, Yoshida A, Nyberg F, Ueda (2000) Vzg-1/lysophosphatidic acid-receptor involved in peripheral pain transmission. *Brain Res Mol Brain Res*. **75**: 350-4.

Roberson DP, Gudes S, Sprague JM, Patoski HA, Robson VK, Blasl F, Duan B, Oh SB, Bean BP, Ma Q, Binshtok AM, Woolf CJ. (2013) Activity-dependent silencing reveals functionally distinct itch-generating sensory neurons. *Nat Neurosci*. **16**: 910-8.

Rohács T, Lopes CM, Michailidis I, Logothetis DE. (2005) PI(4,5)P2 regulates the activation and desensitization of TRPM8 channels through the TRP domain. *Nat Neurosci*. 8: 626-34.

Rothman S. (1941) Physiology of Itching. *Physiol Rev*. **21**: 357-381.

Salas MM, Hargreaves KM, Akopian AN. (2009) TRPA1-mediated responses in trigeminal sensory neurons: interaction between TRPA1 and TRPV1. *Eur J Neurosci*. **29**: 1568-78.

Shim WS, Tak MH, Lee MH, Kim M, Kim M, Koo JY, Lee CH, Kim M, Oh U. (2007) TRPV1 mediates histamine-induced itching via the activation of phospholipase A2 and 12-lipoxygenase. *J Neurosci*. **27**: 2331-7.

Shimada SG, LaMotte RH. (2008) Behavioral differentiation between itch and pain in mouse. *Pain*. **139**: 681-7.

Sikand P, Shimada SG, Green BG, LaMotte RH. (2011) Sensory responses to injection and punctate application of capsaicin and histamine to the skin. *Pain*. **152**: 2485-94.

Taylor-Clark TE, Undem BJ, Macglashan DW Jr, Ghatta S, Carr MJ, McAlexander MA. (2008) Prostaglandin-induced activation of nociceptive neurons via direct interaction with transient receptor potential A1 (TRPA1). *Mol Pharmacol.* **73**: 274-81.

Tigyi G. (2010) Aiming drug discovery at lysophosphatidic acid targets. *Br J Pharmacol*. **161**: 241-70.

Tominaga M, Caterina MJ, Malmberg AB, Rosen TA, Gilbert H, Skinner K, Raumann BE, Basbaum AI, Julius D. (1998) The cloned capsaicin receptor integrates multiple pain-producing stimuli. *Neuron*. **21**: 531-43.

Twycross R, Greaves MW, Handwerker H, Jones EA, Libretto SE, Szepietowski JC, Zylicz Z. (2003) Itch: scratching more than the surface. *QJM*. **96**: 7-26.

Wikström B, Gellert R, Ladefoged SD, Danda Y, Akai M, Ide K, Ogasawara M, Kawashima Y, Ueno K, Mori A, Ueno Y. (2005) Kappa-opioid system in uremic pruritus: multicenter, randomized, double-blind, placebo-controlled clinical studies. *J Am Soc Nephrol*. **16**: 3742-7.

Williams JR, Khandoga AL, Goyal P, Fells JI, Perygin DH, Siess W, Parrill AL, Tigyi G, Fujiwara Y. (2009) Unique ligand selectivity of the GPR92/LPA5 lysophosphatidate receptor indicates role in human platelet activation. *J Biol Chem.* **284**: 17304-19.

Wilson SR, Gerhold KA, Bifolck-Fisher A, Liu Q, Patel KN, Dong X, Bautista DM. (2011) TRPA1 is required for histamine-independent, Mas-related G protein-coupled receptor-mediated itch. *Nat Neurosci*. **14**: 595-602.

Wilson SR, Nelson AM, Batia L, Morita T, Estandian D, Owens DM, Lumpkin EA, Bautista DM. (2013a) The ion channel TRPA1 is required for chronic itch. *J Neurosci*. **33**: 9283-94.

Wilson SR, Thé L, Batia LM, Beattie K, Katibah GE, McClain SP, Pellegrino M, Estandian DM, Bautista DM. (2013b) The epithelial cell-derived atopic dermatitis cytokine TSLP activates neurons to induce itch. *Cell*. **155**: 285-95.

Winter Z, Buhala A, Ötvös F, Jósvay K, Vizler C, Dombi G, Szakonyi G, Oláh Z. (2013) Functionally important amino acid residues in the transient receptor potential vanilloid 1 (TRPV1) ion channel--an overview of the current mutational data. *Mol Pain*. **22**; 9:30.

Yoshioka T, Imura K, Asakawa M, Suzuki M, Oshima I, Hirasawa T, Sakata T, Horikawa T, Arimura A. (2009) Impact of the Gly573Ser substitution in TRPV3 on the development of allergic and pruritic dermatitis in mice. *J Invest Dermatol*. **129**: 714-22.

Zurborg S, Yurgionas B, Jira JA, Caspani O, Heppenstall PA. (2007) Direct activation of the ion channel TRPA1 by Ca2+. *Nat Neurosci.* **10**: 277-9.

.

7. Table and Figure Legends

Table 1. Primer sets for mouse TRPA1 lysine/arginine mutations.

Figure 1. LPA-induced scratching and wiping behaviors in mice.

Scratching (a) and wiping (b) behaviors induced by vehicle or LPA (100 nmol/10 μl) injection into the right cheek of WT mice over 30 min observation. Time courses of scratching (c) and wiping (d) behaviors. A peak of scratching was observed at 16 - 20 min. n ≥ 17 per group. *$p < 0.05$. **$p < 0.01$. Group data are represented as means ± sem.

Figure 2. Effects of LPA on cytosolic Ca^{2+} concentrations in mouse DRG neurons.

(a) Representative traces of increased intracellular Ca^{2+} concentrations ($[Ca^{2+}]_i$) in DRG neurons upon application of 5 μM LPA. (b) Percentage of the LPA-responding (LPA^+) DRG neurons (45.2 ± 5.5 %, 213/500 neurons). (c, d) LPA dose-dependent curves for percentages of LPA^+ neurons (c) and ΔF_{Norm} (see Methods and Materials) in the LPA^+ neurons (d). EC_{50} values are 3.34 and 1.07 μl, respectively. Group data are represented as means ± sem.

Figure 3. LPA-induced $[Ca^{2+}]_i$ increases in mouse DRG neurons are dependent on extracellular calcium and the expression of TRPA1 and/or TRPV1.

(a) Representative traces of $[Ca^{2+}]_i$ change when the extracellular bath solution was Ca^{2+}-free. (b) Representative traces of $[Ca^{2+}]_i$ change in responses to AITC (100 μM), capsaicin (1 μM), KCl (100 mM) and ionomycin (5 μM) after LPA (5 μM). (c) Venn diagram of the classified DRG neurons. Among the LPA^+ neurons (213 neurons),

87.2 ± 2.7 % (184 neurons) expressed TRPA1 and/or TRPV1. (d) LPA-induced increases of ΔF_{Norm} values in $LPA^+/TRPA1^+/TRPV1^+$, $LPA^+/TRPA1^+$, $LPA^+/TRPV1^+$ and LPA^+ alone groups. n ≥ 29 neurons. (e) Time to peak of LPA-induced increases of ΔF_{Norm} values in the same subpopulations. Group data are represented as means ±sem.

Figure 4. Dependence of the LPA^+-DRG neurons on TRPA1 and TRPV1.

(a) The LPA-induced $[Ca^{2+}]_i$ increases were partially inhibited by A967079 (1 μM). (b) The LPA-induced $[Ca^{2+}]_i$ increases were partially inhibited by capsazepine (10 μM). (c and d) The proportion of the LPA^+-DRG neuron are significantly decreased by A967079 (c) or capsazepine (d). (e) LPA^+-DRG neurons were significantly reduced in DRG neurons isolated from TRPA1KO (144/579), TRPV1KO (93/443) and TRPA1/TRPV1 double KO (A1V1DKO) (65/455) mice. $*p < 0.05$. n ≥ 3 per group. Group data are represented as means ± sem.

Figure 5. Dependence of the LPA-induced scratching behaviors on TRPA1 and TRPV1.

Scratching (a) and wiping (b) behaviors induced by vehicle injection into WT mice and LPA (100 nmol/10 μl) injection into WT, TRPA1KO, TRPV1KO and A1V1DKO mice. n ≥ 9 per group. Time courses of scratching (c) and wiping (d) behaviors. Group data are represented as means ± sem.

Figure 6. LPA-induced $[Ca^{2+}]_i$ increases in mouse DRG neurons are inhibited by H2L 5765834, an antagonist of LPA_1, LPA_3 and LPA_5.

(a) Representative traces of $[Ca^{2+}]_i$ changes showing that H2L 5765834 (10μM) inhibits the LPA-induced $[Ca^{2+}]_i$ increases in DRG neurons. (b) Percentages of the LPA-responding neurons during the application of LPA alone and LPA with H2L 5765834. n = 4 per group. *$p < 0.05$. Group data are represented as means ± sem. (c) Venn diagram of the classified DRG neurons. LPA-induced $[Ca^{2+}]_i$ increases are inhibited in 78.0 ± 6.8 % of the LPA^+ neurons (79/95 neurons) by H2L 5765834, 71.5 ± 4.3 %of which (61/79) express TRPA1 and/or TRPV1.

Figure 7. H2L 5765834 dosen't inhibit the $[Ca^{2+}]_i$ increases induced by AITC or capsaicin in mouse DRG neurons.

Representative traces of $[Ca^{2+}]_i$ changes when H2L 5765834 (10 μM) is applied with AITC (100 μM) (a) or capsaicin (1 μM) (b). (c) Percentages of neurons that responded to AITC with H2L 5765834 (61.9 ± 5.4%, 159/247) or capsaicin with H2L 5765834 (74.1 ± 3.0%, 149/201). n = 3 per group. Group data are represented as means ± sem.

Figure 8. Direct activation of mouse TRPA1 by LPA in a membrane-limited manner.

(a) Representative single channel currents induced by LPA (1, 5, 10 μM) in a patch membrane excised from an mTRPA1 expressing HEK293T cell (*lower trace*). Upper two magnified traces are single channel currents observed during LPA application (5 μM (*left*) and 10 μM (*right*)). LPA-induced single channel openings of mTRPA1 are dose-dependent (*upper left*). (b) Representative single-channel currents that were activated by LPA (5 μM) and inhibited by a selective TRPA1 blocker, A967079 (1 μM).

(c) Unitary single-channel current amplitude of mTRPA1 activated by AITC (100 μM) (3.31 ± 0.73 pA) and LPA (5 μM) (3.74 ± 0.55 pA). $n \geq 4$ per group. Group data are represented as means ± sem.

Figure 9. Targeted amino acid residues of mouse TRPA1 channel.

Abbreviated domain structure of mTRPA1 is shown, representing large N-terminal ankyrin repeats (green), six transmembrane domains (blue) and a possible TRP box (purple). Amino acid sequences shown in upper and lower sides of the domain structure are extracted from mTRPA1. These sequences are located in the N- and C-terminal regions close to the transmembrane region. Red letters represent basic amino acid residues; those that were mutated to glutamines in this study are bold and underline. Blue letters represent residues composing transmembrane domains.

Figure 10. KK672-673 and KR977-978 were responsible for the LPA action on mouse TRPA1.

(a) A brief domain structure of mTRPA1. Red stars indicate responsible residues and red circles indicate other examined basic residues. Red arrows indicate four PH-like domains. (b) NP_o values of mutant mTRPA1 channel activation during LPA (5 μM) application. A K592Q mutant was non-functional. $n \geq 3$ per group. $^{**}P < 0.01$ by Welch's t-test. Group data are represented as means ± sem. (c) A representative recording of a KK672-673QQ mutant channel. After application LPA, TRPA1 agonists, carvacrol (500 μM) and (100 μM) were applied. Magnified initial trace and after application of LPA, carvacrol and AITC are also shown.

8. Table and figures

Table 1

Primer sets for mouse TRPA1 lysine/arginine mutations

mTRPA1 mutant	Sense primer (5' → 3')	Antisense primer (5' → 3')
K592Q	GCCCTGCACAATcAGCGCAAGGAAGTG	CACTTCCTTGCGCTgATTGTGCAGGGC
R593Q	CTGCACAATAAGCaaAAGGAAGTGGTT	AACCACTTCCTTttGCTTATTGTGCAG
K594Q	CACAATAAGCGCcAGGAAGTGGTTCTC	GAGAACCACTTCCTgGCGCTTATTGTG
R602Q	CTCACAACCATCcaAAATAAAAGATGG	CCATCTTTTATTTtgGATGGTTGTGAG
K604Q	ACCATCAGAAATcAAAGATGGGATGAG	CTCATCCCATCTTTgATTTCTGATGGT
R605Q	ATCAGAAATAAAcaATGGGATGAGTGT	ATCAGAAATAAAcaATGGGATGAGTGT
KK672-673QQ	TCCATGACCcAAcAAGTAGCACCTACC	GTGCTACTTgTTgGGTCATGGATAATGG
KK799-800QQ	TCCAACAGcAAcaGAATTACTTCCTG	AATTCtgTTgCTGTTGGAAAATTTGG
K972Q	GAGGTCCAGcAGCATGCGTCAT	ATGACGCATGCTgCTGGACCTC
KK977-978QQ	CATGCGTCATTGcAGcaGATTGCTATGC	GCATAGCAATCtgCTgCAATGACGCATG
KK991-992QQ	CAACTTAGAAcAAcAGCTGCCACTC	GAGTGGCAGCTgTTgTTCTAAGTTG
RK999-1000QQ	CTGGTACTTACagcAAGTGGATCAG	CTGATCCACTTgctGTAAGTACCAG
R1004Q	GTGGATCAGcaGTCCACCATCG	CGATGGTGGACtgCTGATCCAC
R1012Q	GTATCCAAATcaACCCAGGCACG	CGTGCCTGGGTtgATTTGGATAC
R1014Q	CAAATAGACCCcaGCACGGCAGG	CCTGCCGTGCtgGGGTCTATTTG
R1017Q	CCAGGCACGGCcaGATGCTACGG	CCGTAGCATCtgGCCGTGCCTGG
R1020Q	CAGGATGCTAcaGTTTTTTCATTAC	GTAATGAAAAAACtgTAGCATCCTG
R1092Q	TCTTTCCAAGACcaGTTCAAGAAGGAG	CTCCTTCTTGAACtgGTCTTGGAAAGA
K1094Q	CAAGACAGGTTCcAaAAGGAGAGGCTG	CAGCCTCTCCTTtTgGAACCTGTCTTG
K1095Q	GACAGGTTCAAGcAaGAGAGGCTGGAA	TTCCAGCCTCTCtTgCTTGAACCTGTC
R1097Q	TTCAAGAAGGAGcaGCTGGAACAGATG	CATCTGTTCCAGCtgCTCCTTCTTGAA

Lowercase letters indicate substituted nucleotides.

Figure 1

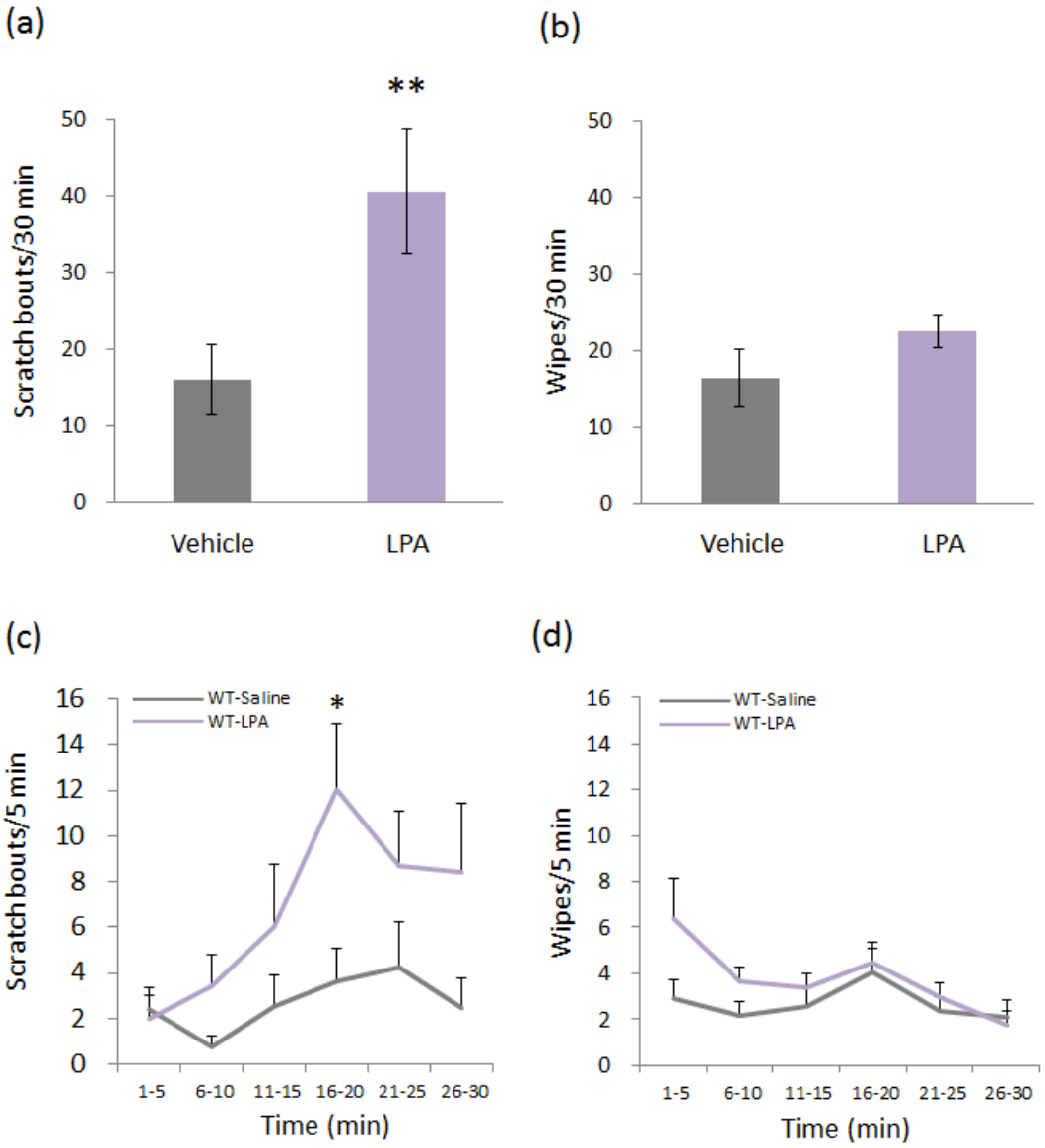
(a)
**
Scratch bouts/30 min
50
40
30
20
10
0
Vehicle
LPA
(b)
Wipes/30 min
50
40
30
20
10
0
Vehicle
LPA
(c)
WT-Saline
WT-LPA
*
Scratch bouts/5 min
16
14
12
10
8
6
4
2
0
1-5
6-10
11-15
16-20
21-25
26-30
Time (min)
(d)
WT-Saline
WT-LPA
Wipes/5 min
16
14
12
10
8
6
4
2
0
1-5
6-10
11-15
16-20
21-25
26-30
Time (min)

Figure 2

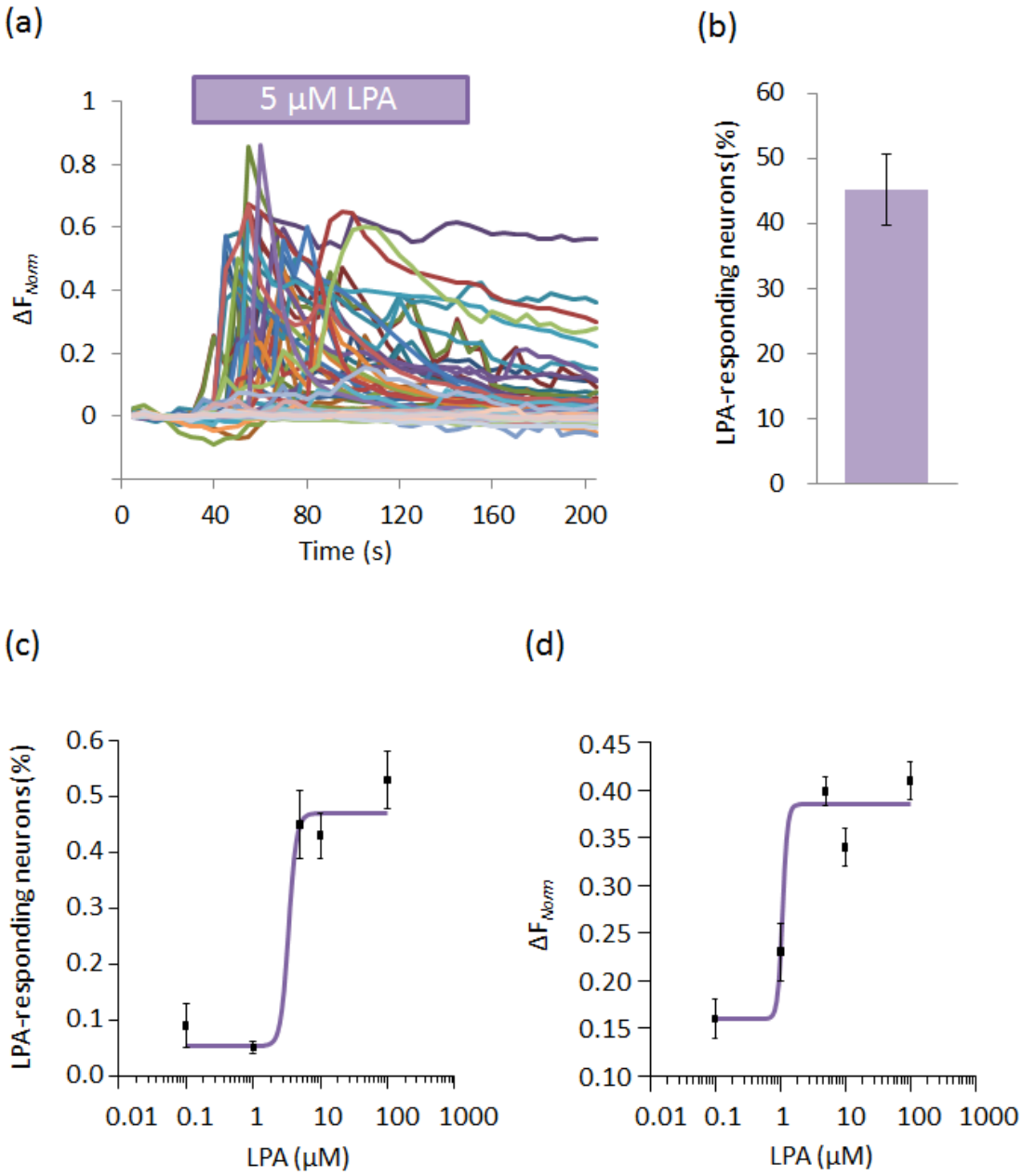
(a)
5 μM LPA
ΔF Norm
Time (s)
(b)
LPA-responding neurons(%)
(c)
LPA-responding neurons(%)
LPA (μM)
(d)
ΔF Norm
LPA (μM)

Figure 3

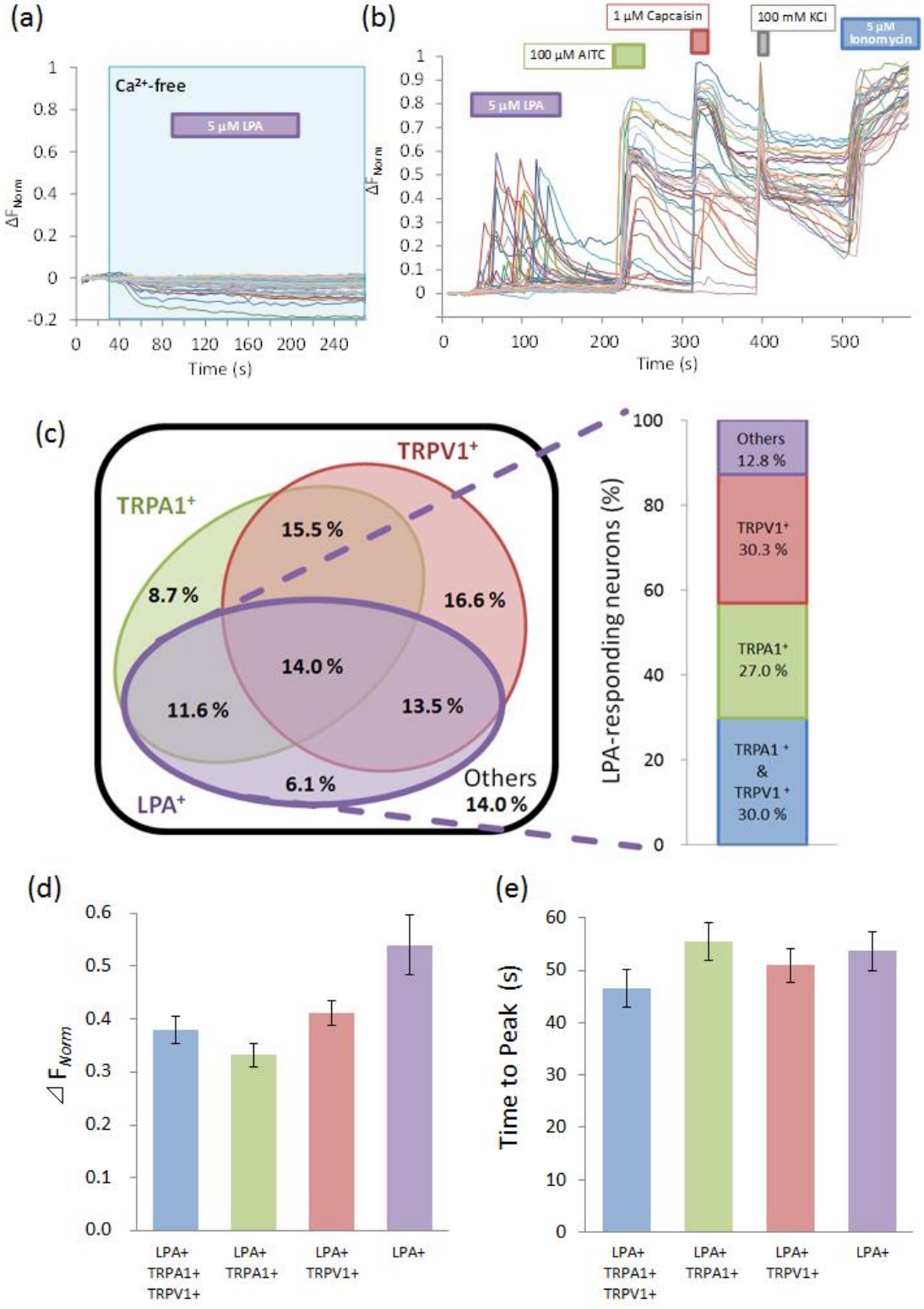
(a)
Ca²⁺-free
5 μM LPA
ΔF Norm
Time (s)
(b)
1 μM Capcaisin
100 mM KCl
5 μM Ionomycin
100 μM AITC
5 μM LPA
ΔF Norm
Time (s)
(c)
TRPV1⁺
TRPA1⁺
LPA⁺
15.5 %
8.7 %
16.6 %
14.0 %
11.6 %
13.5 %
6.1 %
Others
14.0 %
LPA-responding neurons (%)
Others
12.8 %
TRPV1⁺
30.3 %
TRPA1⁺
27.0 %
TRPA1⁺
&
TRPV1⁺
30.0 %
(d)
ΔF Norm
LPA+ TRPA1+ TRPV1+
LPA+ TRPA1+
LPA+ TRPV1+
LPA+
(e)
Time to Peak (s)
LPA+ TRPA1+ TRPV1+
LPA+ TRPA1+
LPA+ TRPV1+
LPA+

Figure 4

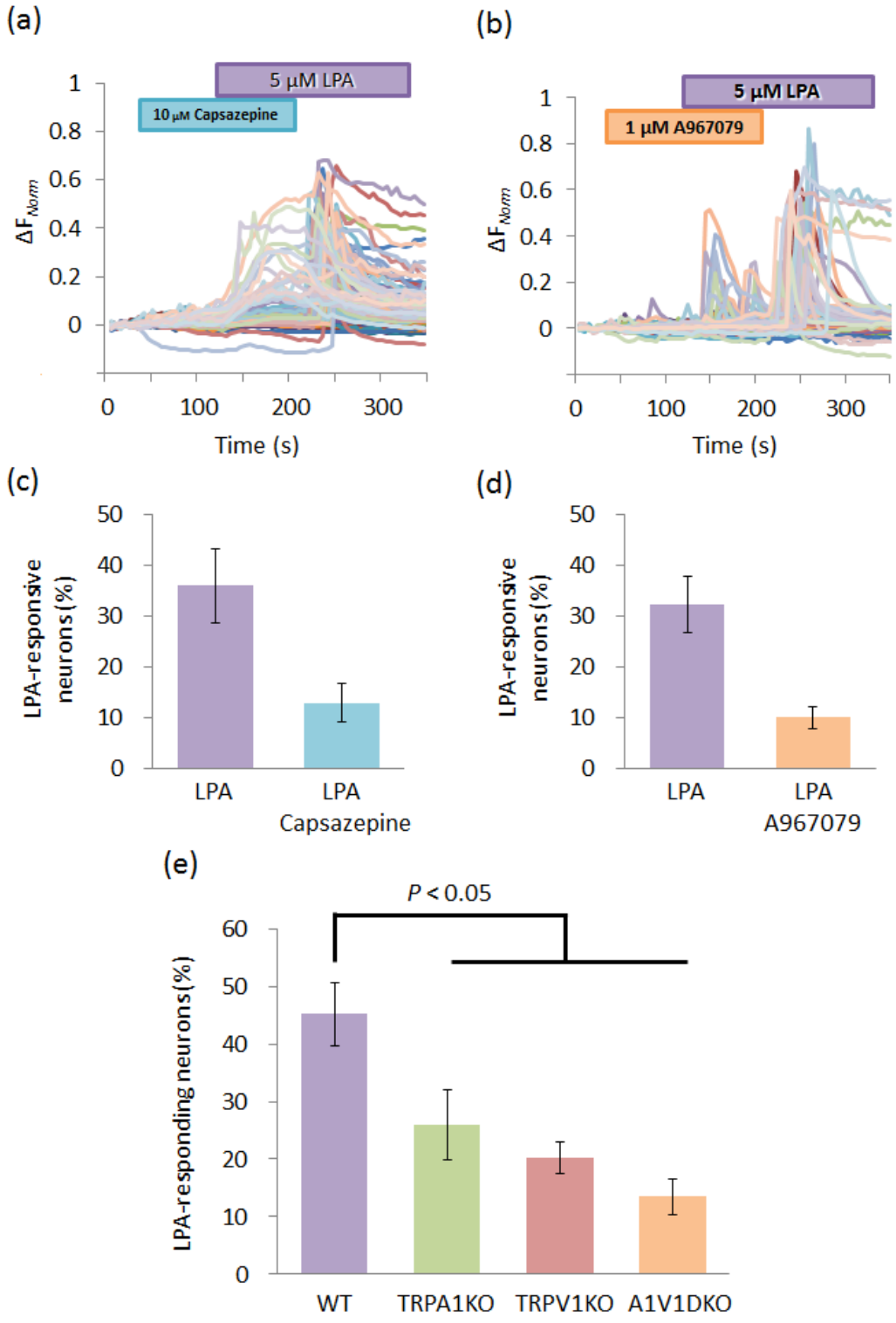
(a)
5 μM LPA
10 μM Capsazepine
ΔF Norm
Time (s)
(b)
5 μM LPA
1 μM A967079
ΔF Norm
Time (s)
(c)
LPA-responsive neurons (%)
LPA
LPA Capsazepine
(d)
LPA-responsive neurons (%)
LPA
LPA A967079
(e)
P < 0.05
LPA-responding neurons (%)
WT
TRPA1KO
TRPV1KO
A1V1DKO

Figure 5

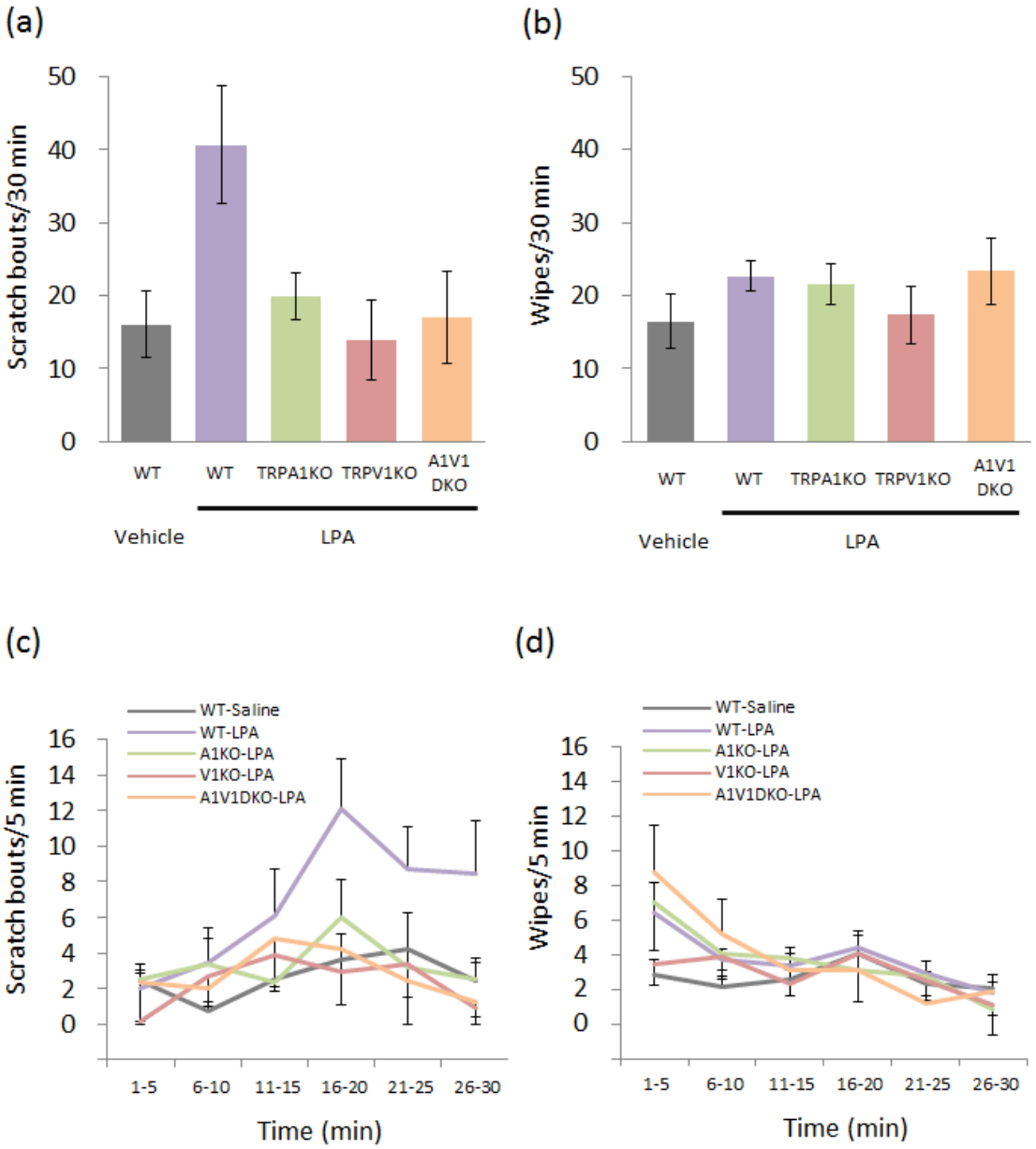
(a)
Scratch bouts/30 min
50
40
30
20
10
0
WT
WT
TRPA1KO
TRPV1KO
A1V1 DKO
Vehicle
LPA
(b)
Wipes/30 min
50
40
30
20
10
0
WT
WT
TRPA1KO
TRPV1KO
A1V1 DKO
Vehicle
LPA
(c)
Scratch bouts/5 min
WT-Saline
WT-LPA
A1KO-LPA
V1KO-LPA
A1V1DKO-LPA
16
14
12
10
8
6
4
2
0
1-5
6-10
11-15
16-20
21-25
26-30
Time (min)
(d)
Wipes/5 min
WT-Saline
WT-LPA
A1KO-LPA
V1KO-LPA
A1V1DKO-LPA
16
14
12
10
8
6
4
2
0
1-5
6-10
11-15
16-20
21-25
26-30
Time (min)

Figure 6

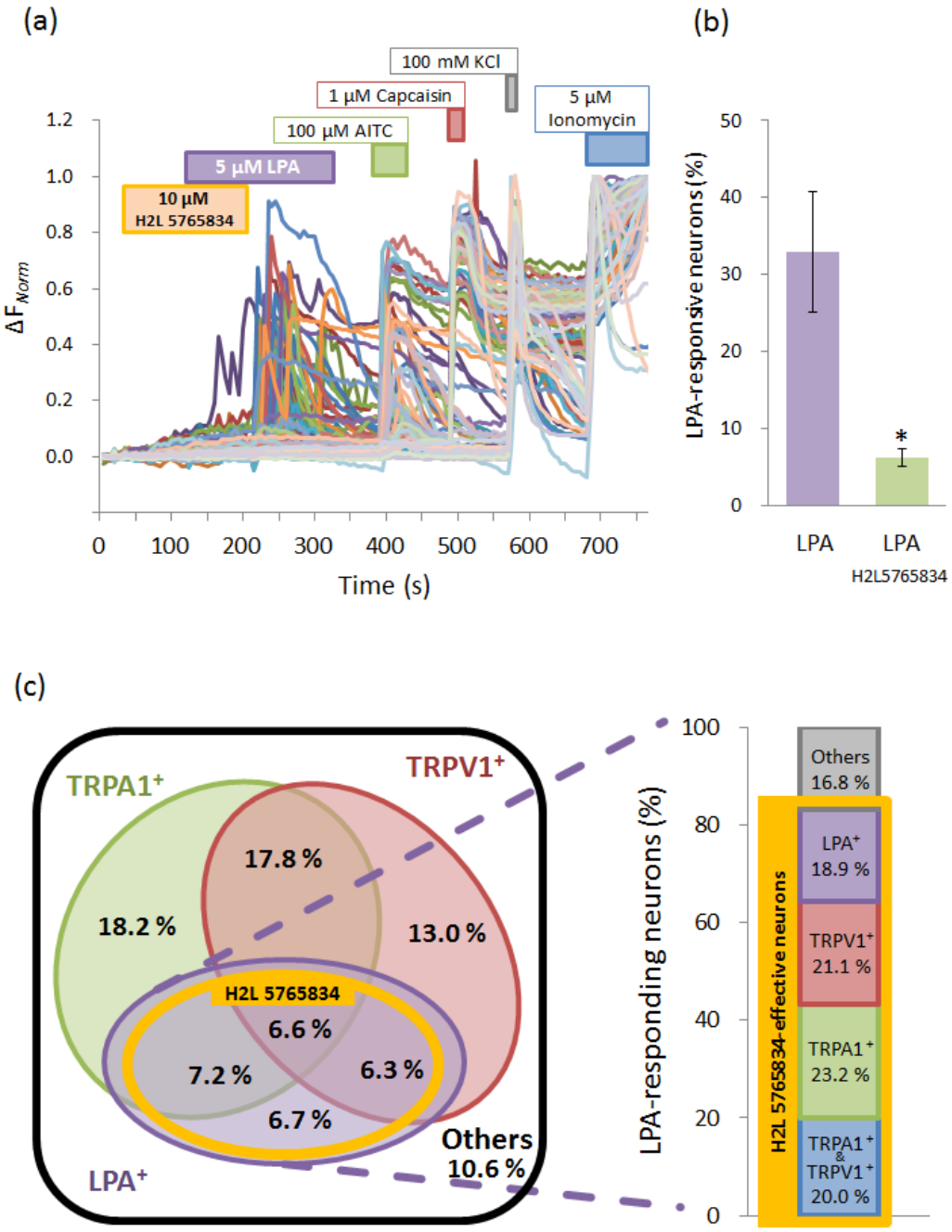
(a)
100 mM KCl
1 µM Capcaisin
100 µM AITC
5 µM Ionomycin
5 µM LPA
10 µM H2L 5765834
ΔF Norm
Time (s)
(b)
LPA-responsive neurons (%)
LPA
LPA H2L5765834
(c)
TRPA1+
TRPV1+
LPA+
17.8 %
18.2 %
13.0 %
H2L 5765834
6.6 %
7.2 %
6.3 %
6.7 %
Others 10.6 %
LPA-responding neurons (%)
H2L 5765834-effective neurons
Others 16.8 %
LPA+ 18.9 %
TRPV1+ 21.1 %
TRPA1+ 23.2 %
TRPA1+ & TRPV1+ 20.0 %

Figure 7

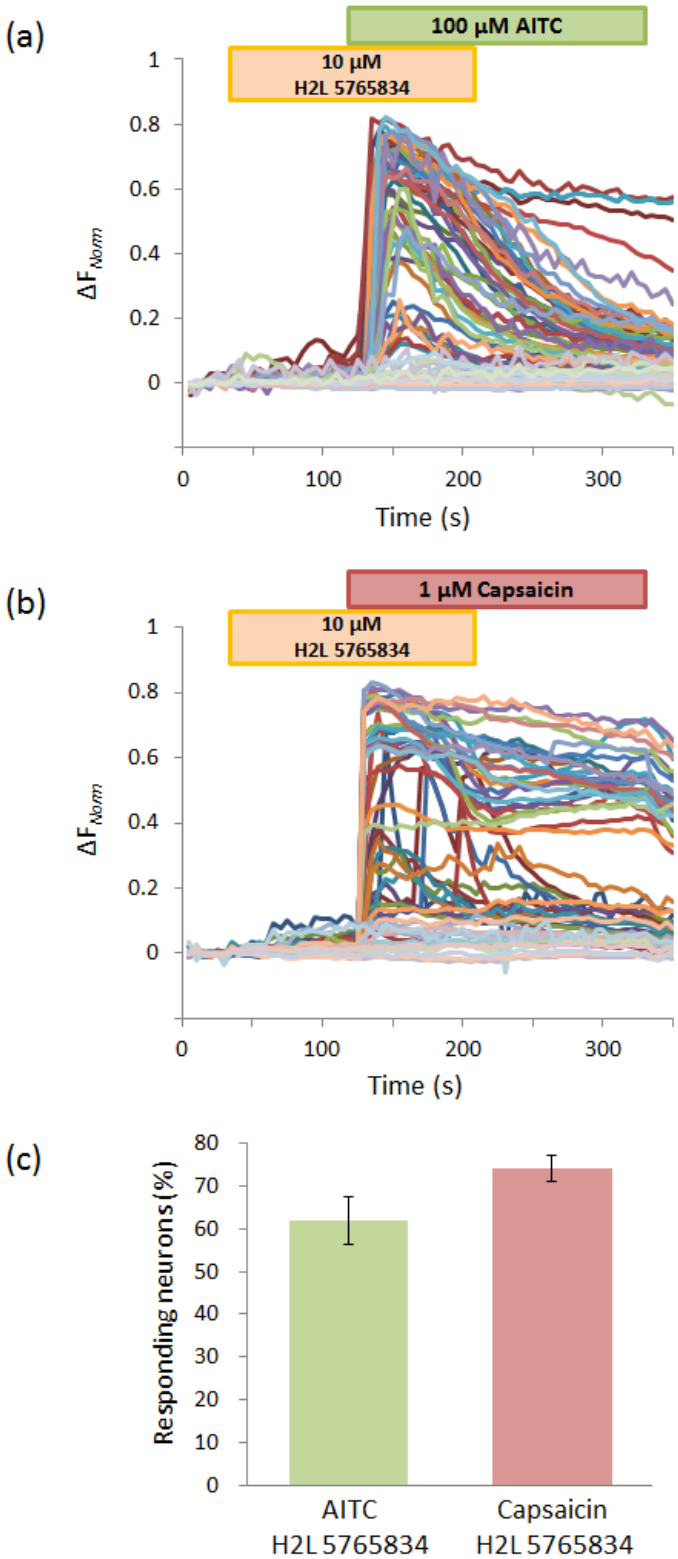
(a)
100 µM AITC
10 µM
H2L 5765834
ΔF Norm
Time (s)
(b)
1 µM Capsaicin
10 µM
H2L 5765834
ΔF Norm
Time (s)
(c)
Responding neurons (%)
AITC
H2L 5765834
Capsaicin
H2L 5765834

Figure 8

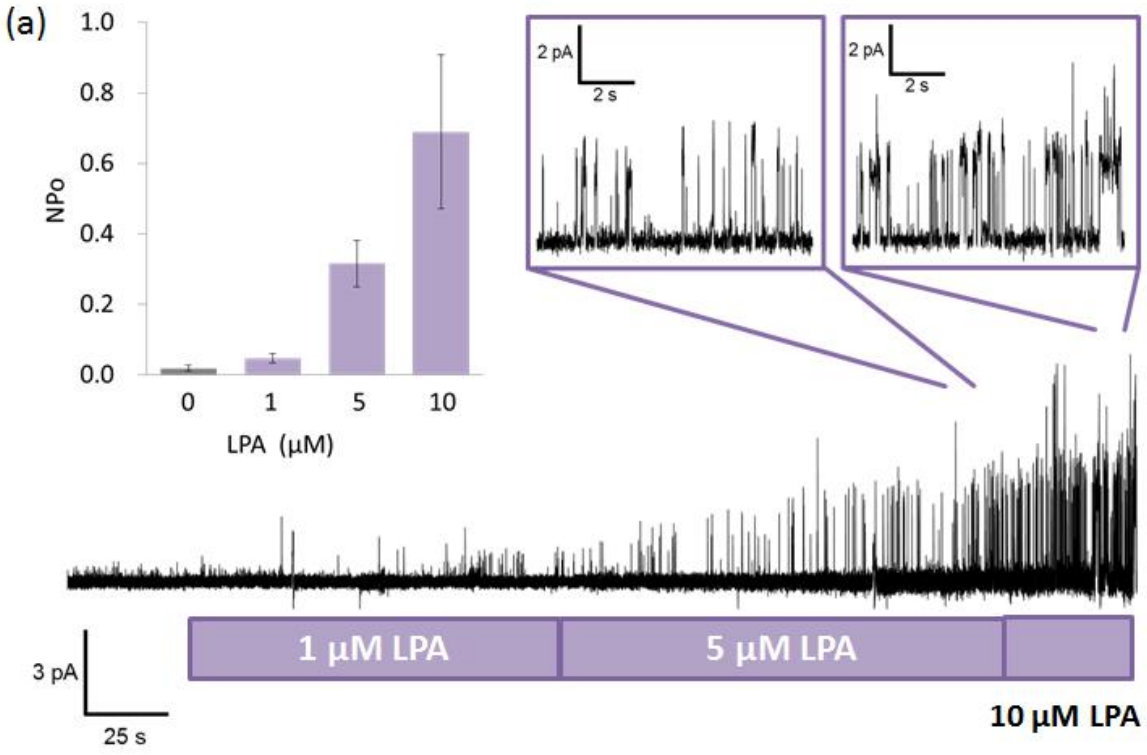
(a)
1.0
0.8
0.6
0.4
0.2
0.0
NPo
0
1
5
10
LPA (μM)
2 pA
2 s
2 pA
2 s
1 μM LPA
5 μM LPA
10 μM LPA
3 pA
25 s

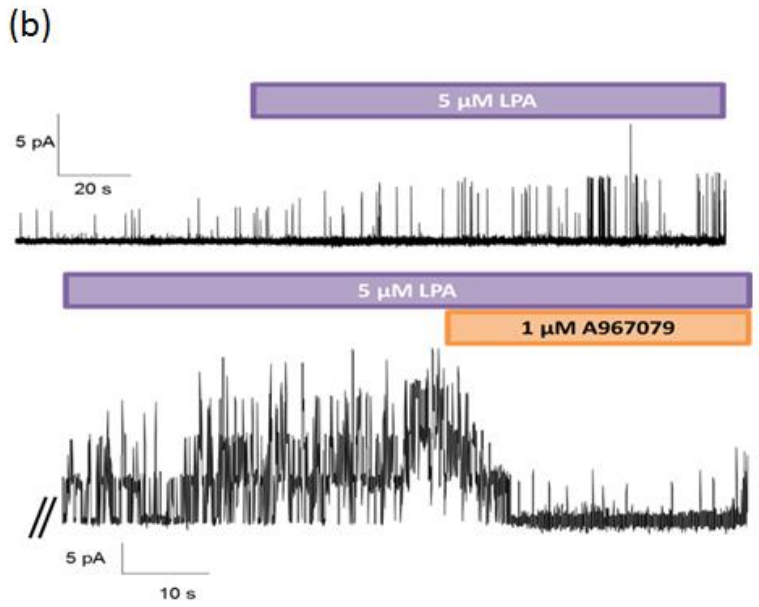
(b)
5 μM LPA
5 pA
20 s
5 μM LPA
1 μM A967079
5 pA
10 s

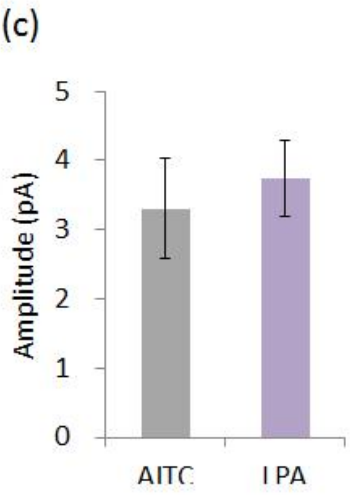
(c)
Amplitude (pA)
5
4
3
2
1
0
AITC
LPA

Figure 9

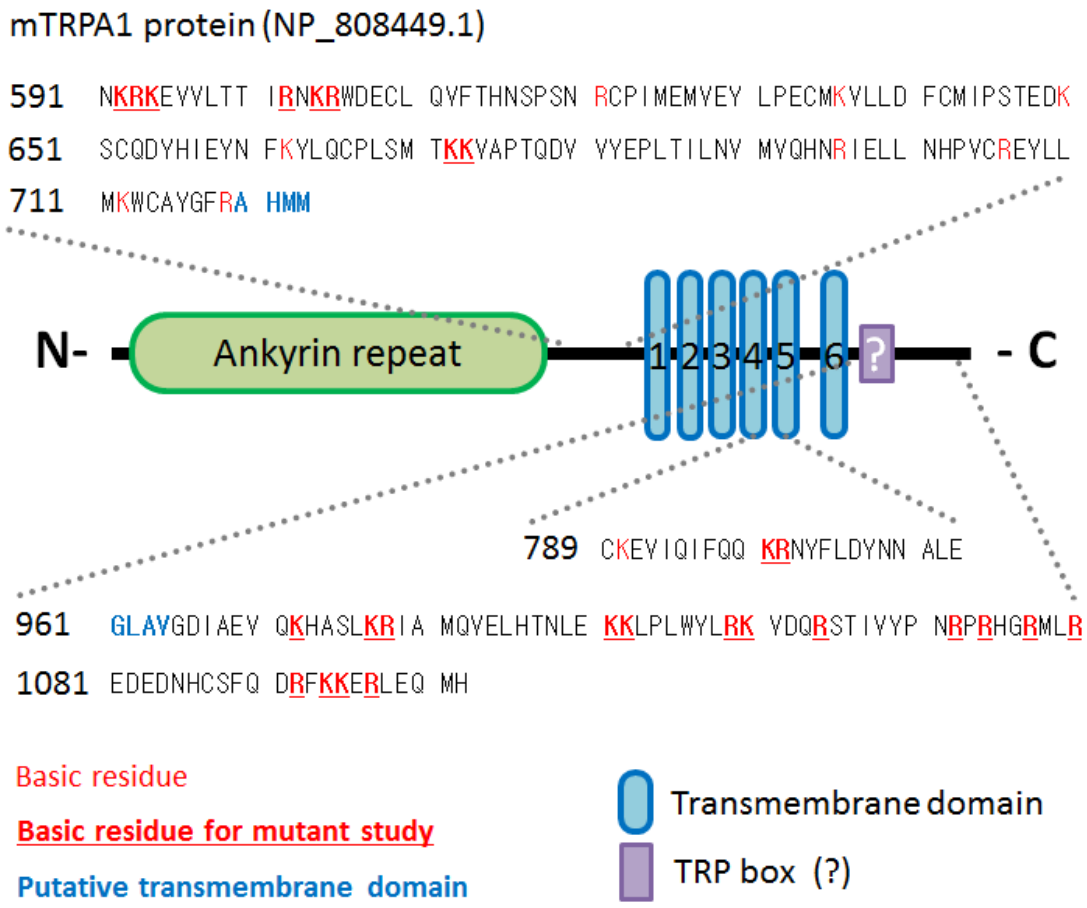
mTRPA1 protein (NP_808449.1)
591 NKRKEVVLTT IRNKRWDECL QVFTHNSPSN RCPIMEMVEY LPECMKVLLD FCMIPSTEDK
651 SCQDYHIEYN FKYLQCPLSM TKKVAPTQDV VYEPLTILNV MVQHNRIELL NHPVCREYLL
711 MKWCAYGFRA HMM
N-
Ankyrin repeat
1 2 3 4 5 6 ?
- C
789 CKEVIQIFQQ KRNYFLDYNN ALE
961 GLAVGDIAEV QKHASLKRIA MQVELHTNLE KKLPLWYLRK VDQRSTIVYP NRPRHGRMLR
1081 EDEDNHCSFQ DRFKKERLEQ MH
Basic residue
Basic residue for mutant study
Putative transmembrane domain
Transmembrane domain
TRP box (?)

Figure 10

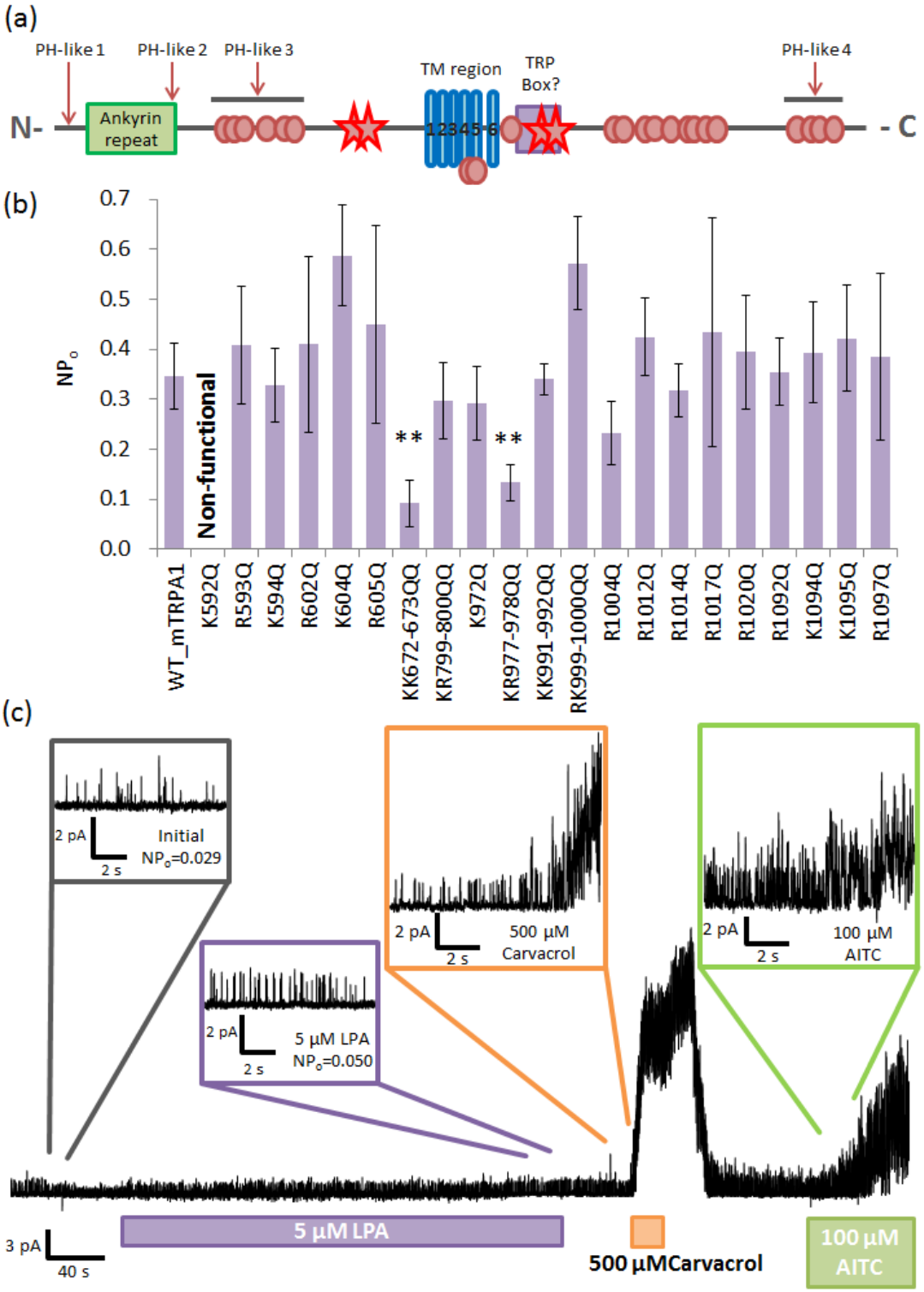
(a)
PH-like 1
PH-like 2
PH-like 3
TM region
TRP Box?
PH-like 4
N-
Ankyrin repeat
1 2 3 4 5 6
- C
(b)
NPo
0.7
0.6
0.5
0.4
0.3
0.2
0.1
0.0
Non-functional
**
**
WT_mTRPA1
K592Q
R593Q
K594Q
R602Q
K604Q
R605Q
KK672-673QQ
KR799-800QQ
K972Q
KR977-978QQ
KK991-992QQ
RK999-1000QQ
R1004Q
R1012Q
R1014Q
R1017Q
R1020Q
R1092Q
K1094Q
K1095Q
R1097Q
(c)
2 pA
2 s
Initial
NPo=0.029
2 pA
2 s
5 μM LPA
NPo=0.050
2 pA
2 s
500 μM
Carvacrol
2 pA
2 s
100 μM
AITC
3 pA
40 s
5 μM LPA
500 μMCarvacrol
100 μM
AITC

9. Acknowledgements

I greatly thank to Dr. Makoto Tominaga for tremendous supports for this study overall. I thank Dr. Kunitoshi Uchida for a lot of experimental instruction and valuable discussions, and Naomi Fukuta and Claire Saito for constructing mTRPA1 mutants. I thank Dr. David Julius (University of California, San Francisco) for generously providing both TRPA1KO and TRPV1KO mice. I thank all members of the laboratory of Cell Signaling for many helpful discussion and comments.